

An exactly solvable model for nonlinear resonant scattering

This article has been downloaded from IOPscience. Please scroll down to see the full text article.

2012 Nonlinearity 25 2473

(<http://iopscience.iop.org/0951-7715/25/9/2473>)

View [the table of contents for this issue](#), or go to the [journal homepage](#) for more

Download details:

IP Address: 70.199.195.32

The article was downloaded on 03/08/2012 at 13:43

Please note that [terms and conditions apply](#).

An exactly solvable model for nonlinear resonant scattering

Stephen P Shipman¹ and Stephanos Venakides²

¹ Department of Mathematics, Louisiana State University, Lockett Hall 303; Baton Rouge, LA 70803, USA

² Department of Mathematics, Duke University, Box 90320; Durham, NC 27708, USA

E-mail: shipman@math.lsu.edu and ven@math.duke.edu

Received 4 March 2012, in final form 6 June 2012

Published 3 August 2012

Online at stacks.iop.org/Non/25/2473

Recommended by J Lega

Abstract

This work analyses the effects of cubic nonlinearities on certain resonant scattering anomalies associated with the dissolution of an embedded eigenvalue of a linear scattering system. These sharp peak-dip anomalies in the frequency domain are often called Fano resonances. We study a simple model that incorporates the essential features of this kind of resonance. It features a linear scatterer attached to a transmission line with a point-mass defect and coupled to a nonlinear oscillator. We prove two power laws in the small coupling ($\gamma \rightarrow 0$) and small nonlinearity ($\mu \rightarrow 0$) regime. The asymptotic relation $\mu \sim C\gamma^4$ characterizes the emergence of a small frequency interval of triple harmonic solutions near the resonant frequency of the oscillator. As the nonlinearity grows or the coupling diminishes, this interval widens and, at the relation $\mu \sim C\gamma^2$, merges with another evolving frequency interval of triple harmonic solutions that extends to infinity. Our model allows rigorous computation of stability in the small μ and γ limit. The regime of triple harmonic solutions exhibits bistability—those solutions with largest and smallest response of the oscillator are linearly stable and the solution with intermediate response is unstable.

Mathematics Subject Classification: 70K30, 70K40, 70K42, 70K50

(Some figures may appear in colour only in the online journal)

1. Introduction of the nonlinear model

The interaction between a resonant scatterer and an extended system that admits a spectral continuum of states is a fundamental problem in classical and quantum systems. A variety

of simple models have been devised to elucidate this interaction, and they have the advantage of providing clean mathematical treatments of specific phenomena. Lamb [8] observed in 1900 that, if a simple harmonic oscillator is attached to a point on a string, the loss of energy by radiation into the string effectively results in the usual damped oscillator. Komech [7] extended the analysis to a general simple nonlinear oscillator and proved that finite-energy solutions tend to an equilibrium state of the oscillator and in fact that transitions between any two equilibrium states are possible. In the frequency domain, resonance effects of an oscillator on extended time-harmonic states were treated by Fano [4], in order to explain peak-dip anomalies (the ‘Fano line shape’) observed in the scattering of electrons by the noble gases. These sharp resonances are a result of a weak coupling of a bound state to a continuum of extended states. The frequency of the bound state is realized as an eigenvalue of the equations of the extended system, embedded in the continuous spectrum, and this eigenvalue is unstable with respect to perturbations of the system. An analogous phenomenon occurs in the scattering of an EM plane wave by a photonic crystal slab. Sharp peak-dip anomalies in the transmission of energy across the scatterer (similar to those in figure 2 and often referred to as resonances of Fano type) are due to the resonant excitation, by the incident wave, of the state that is localized in the slab [1, 2, 17]. These resonances can be analysed rigorously by means of a complex-analytic perturbation theory of the scattering problem about the parameters of the bound state, and one obtains asymptotic formulae that reveal fine details of the anomalies [15, 18]. The analysis is applicable quite generally to scattering problems that admit unstable bound states, including continuous as well as lattice models [14, 16].

Kerr (cubic) nonlinearity in models of resonant harmonic scattering have been investigated by several authors, mostly numerically. Its effects on resonance in dielectric slabs is important for applications exploiting tunable bistability [9]. The Fano–Anderson model of a resonator coupled to a single chain of ‘atoms’ with nearest-neighbour interactions exhibits a sharp dip in the transmission coefficient in the middle of the spectrum. When Kerr nonlinearity is introduced into the resonator, a stable scattering state bifurcates as the nonlinearity reaches a critical value, producing multiple scattering solutions and bistability in an interval of resonant frequencies [12, 13]. Discrete nonlinear chains have been proposed for modelling photonic crystal waveguides [10, 11]. When, instead of a single atomic chain, two atomic chains are coupled together, one can construct embedded trapped modes exhibiting the Fano-type anomaly observed in photonic systems, and numerical computations show that Kerr nonlinearity causes intricate multi-valued transmission coefficients [16].

In order to understand the fundamental effects that nonlinearity produces upon resonant scattering through exact explicit formulae, we introduce a dynamical system consisting of two subsystems coupled together (figure 1): (1) a transmission line of Schrödinger type with a point-mass defect acting as a nonresonant scatterer and (2) a nonlinear resonator coupled to the defect on the line. When the nonlinearity is set to zero, the model incorporates the essential features of these linear photonic systems described above inasmuch as the resonant phenomena are concerned. The model elucidates fundamental nonlinear effects that coincide with asymptotic relations between the parameters of coupling and nonlinearity. The use of a discrete transmission line, as in the Fano–Anderson model, in place of a continuous one would have the effect of making the spectrum of finite rather than infinite extent, and is of no consequence for the Fano resonance.

In our model, multiple scattering solutions near the Fano resonance are observed for any value of the parameter λ of the Kerr nonlinearity, if the intensity of the incident field J is large enough so that the composite nonlinearity parameter $\mu = \lambda J^2$ exceeds a certain threshold. Below this threshold, the solution is unique. This is also true for the Fano–Anderson

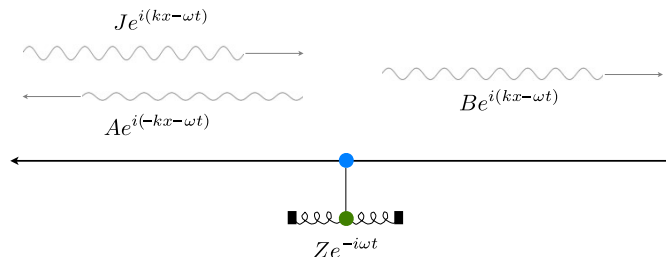


Figure 1. The model for nonlinear resonant scattering. The transmission line models the ambient space, the mass attached to the line models the (nonresonant) scatterer, and the nonlinear oscillator attached to the mass models the bound state, which is responsible for resonance. The Kerr nonlinearity is confined to the oscillator. The elements of a harmonic scattering field at frequency ω correspond to the form (2.2).

model with nonlinearity studied by Miroschnichenko, *et al* [12, 13]. The threshold depends on the coupling γ between the transmission line and the resonator. Weaker coupling requires a smaller value of μ to achieve qualitatively the same nonlinear resonant effects. The asymptotic analysis of the limit $\mu \rightarrow 0, \gamma \rightarrow 0$, gives a precise description of these (fully) nonlinear phenomena and is the focus of our present study.

Asymptotically small coupling pushes the Fano resonance to its singular limit, in which a system that admits an eigenvalue embedded in the continuous spectrum is perturbed, causing the eigenvalue to dissolve [18]. This situation was described by Fano as a ‘configuration interaction’ which causes ‘the mixing of a configuration belonging to a discrete spectrum with continuous spectrum configurations’ [4]. In the regime of weak coupling, extreme amplitude enhancement in the resonator, together with very small Kerr coefficient, causes pronounced nonlinear effects. This paper analyses the delicate balances between two small parameters—the composite nonlinearity parameter μ and the coupling γ . There are two distinguished asymptotic balances, one that characterizes the onset of a frequency band of multiple solutions at the Fano resonance and another that characterizes the merging of this band with a second high-frequency band of multiple solutions. The results are summarized in table 1 and figure 4.

A discussion and comparison with the models of Lamb and Komech as well as the Duffing oscillator is offered in the final section 5. The reader may decide to browse that discussion before embarking on the analysis of our model in sections 2–4.

The transmission line with a point mass at $x = 0$ is the system

$$\begin{aligned} iu_t(x, t) &= -hu_{xx}(x, t), & x \neq 0, \\ iu_t(0, t) &= -\tau(u_x(0^+, t) - u_x(0^-, t)), \end{aligned}$$

in which $h > 0$ carries units of area per time and $\tau > 0$ carries units of length per time. Selecting $\mathcal{T} = h/\tau^2$ and $\mathcal{X} = h/\tau$ as units of time and space nondimensionalizes the equation and removes h and τ . Thus the nondimensional frequency $\omega = 1$ corresponds to the dimensional frequency $2\pi\tau^2/h$. The resonator is a nonlinear harmonic oscillator with cubic, or Kerr, nonlinearity, that obeys the equation in nondimensional form

$$i\dot{z}(t) = E_0z(t) + \lambda|z(t)|^2z(t).$$

The nondimensional characteristic frequency E_0 is relative to the fixed frequency unit $2\pi/\mathcal{T}$, and λ is a nondimensionalization of a parameter carrying units of frequency per square units of z (the values u and z of the fields are assumed to be nondimensionalized relative to a common unit). Neither E_0 nor λ can be eliminated from the equation.

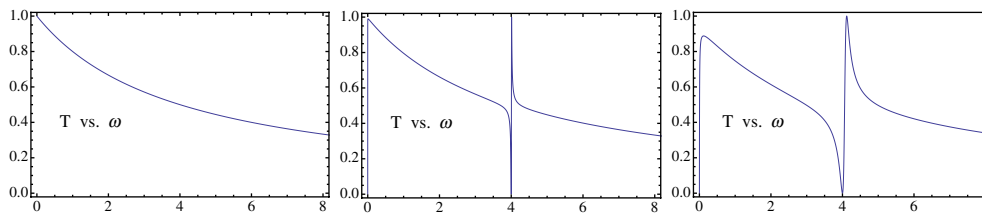


Figure 2. Transmission $T = |B/J|^2$ versus frequency for the linear system ($\lambda = 0$) and normalized incident amplitude $J = 1$ for three values of the coupling parameter γ : From left to right, $\gamma = 0.0, 0.2, 0.7$. The characteristic frequency of the oscillator is $\omega = E_0 = 4$.

These two systems are then coupled by a parameter γ ,

$$\begin{aligned} iu_t(x, t) &= -u_{xx}(x, t), & x &\neq 0 & & \text{(transmission line),} \\ i\dot{y}(t) &= \gamma z(t) - (u_x(0^+, t) - u_x(0^-, t)) & y(t) &= u(0, t) & & \text{(point defect on the line),} \\ i\dot{z}(t) &= E_0 z(t) + \gamma y(t) + \lambda |z(t)|^2 z(t) & & & & \text{(resonator).} \end{aligned} \quad (1.1)$$

Nonlinearity is measured by the composite parameter

$$\mu = \lambda J^2$$

where J is the amplitude of a monochromatic field emanating from a source at $-\infty$ (see figure 1 or (2.2)). In its dimensional form, μ and γ are frequencies, with μ being amplitude-dependent and depending quadratically on the strength of the incident field.

The resonant amplification of the oscillator in the linear system ($\lambda = 0$), accompanied by sharp transmission anomalies near the resonant frequency E_0 , as described above, is portrayed in figure 2. As the coupling γ of the oscillator to the transmission line vanishes, the resonant amplification becomes unbounded. In the limit $\gamma \rightarrow 0$, the motion of the oscillator becomes a bound state for the decoupled system, whose frequency is embedded in the continuous spectrum arising from the transmission line.

The nonlinear system (1.1) admits time-periodic solutions, which the Kerr form $\lambda |z|^2 z$ of the nonlinearity allows to be monochromatic. Even a small nonlinearity has a pronounced effect on the resonance, due to the high-amplitude fields produced. Figure 3 shows how multiple scattering solutions (nonuniqueness of the scattering problem) appear near the resonant frequency and spread to higher frequencies as the nonlinearity parameter is increased. Similarly, a new branch of solutions emerges from the infinite frequency limit and spreads to lower frequencies.

This work proves that the bifurcations occur as portrayed in figure 4, as the nonlinearity increases from the value zero. The analysis reveals characteristic power laws between the coupling parameter γ and the composite parameter of nonlinearity μ in the asymptotic regime of $\gamma \rightarrow 0$ and $\mu \rightarrow 0$ (see table 1 and figure 4). The critical relation $\gamma^4/\mu \sim \text{Const.}$ marks the onset of a narrow frequency interval $[\omega_1, \omega_2]$ of triple solutions near the resonant frequency. For each frequency above this interval and below a high frequency $\omega_3 \sim C\gamma^{-2}$, the system admits a unique harmonic solution. As μ increases relative to γ , the intervals $[\omega_1, \omega_2]$ and $[\omega_3, \infty)$ of triple solutions widen until they merge, that is $\omega_2 = \omega_3 \sim C$, at the critical power law $\gamma^2/\mu \sim \text{Const.}$ For any fixed, small μ and γ , there are at most three frequencies that separate intervals of unicity from intervals of triple solutions; we call these *transition frequencies*. Understanding of the dependence of the transition frequencies ω_1, ω_2 and ω_3 on the parameters γ and μ can be illustrated graphically through the intersection points of two curves in the plane whose coordinates are reparametrizations of the frequency of a harmonic excitation and the ‘response’ of the resonator (section 3).

The stability of multiple scattering solutions is important in applications involving bistable optical transmission [3, 9, 13, 20]. It is commonly understood that, at frequencies for which a nonlinear resonant system admits a unique periodic solution (for a given system and source-field amplitude J), this field is stable under perturbations. At frequencies for which there are exactly three periodic solutions, there should be bistability, that is, two solutions are stable and one unstable, the unstable one being that with intermediate amplitude (see, e.g. the references just cited). The analysis in this section yields precise statements about this kind of bistable behaviour in our model of nonlinear resonance (theorem 2).

2. Harmonic solutions of the nonlinear model

System (1.1) admits harmonic scattering solutions, in which a field $Je^{i(kx-\omega t)}$ oscillating at frequency ω in the string is incident on the resonator from the left (figure 1),

$$\begin{aligned} u(x, t) &= (Je^{ikx} + Ae^{-ikx})e^{-i\omega t}, & x < 0, \\ u(x, t) &= Be^{ikx}e^{-i\omega t}, & x > 0, \\ y(t) &= Be^{-i\omega t}, \\ z(t) &= Ze^{-i\omega t}, \end{aligned} \tag{2.2}$$

where $y(t) = u(0, t)$ represents the state of the defect in the transmission line. The wave number $k > 0$ in the string and the frequency ω are subject to the dispersion relation for the free string $\omega = k^2$. The continuity of u provides the relation

$$J + A = B,$$

and (1.1) reduces to the algebraic system

$$\begin{aligned} (2ik - k^2)B + \gamma Z &= 2ikJ, \\ \gamma B + (E_0 - k^2)Z + \lambda|Z|^2 Z &= 0, \end{aligned}$$

which can be written as a cubic equation for Z/J and a linear relation between B/J and Z/J :

$$\begin{aligned} \frac{2ik\gamma}{2ik - k^2} - \left(\frac{\gamma^2}{2ik - k^2} + k^2 - E_0 \right) \frac{Z}{J} + \lambda J^2 \left| \frac{Z}{J} \right|^2 \frac{Z}{J} &= 0, \\ \frac{B}{J} &= \frac{2ik - \gamma(Z/J)}{2ik - k^2}. \end{aligned} \tag{2.3}$$

We define the transmission coefficient as

$$T = \left| \frac{B}{J} \right|^2.$$

Evidently, the dependence of T on λ and J is only through the composite parameter

$$\mu := \lambda J^2.$$

In figures 3 and 5, one observes two intervals of the ω -line in which the harmonic scattering problem has three solutions and two intervals in which it has one solution. These intervals are separated by three transition frequencies $k_i^2 = \omega_i(\gamma, \mu, E_0)$, $i = 1, 2, 3$:

$$\begin{aligned} (0, \omega_1) \cup (\omega_2, \omega_3) & \quad \text{one solution,} \\ (\omega_1, \omega_2) \cup (\omega_3, \infty) & \quad \text{three solutions.} \end{aligned} \tag{2.4}$$

When μ is decreased or γ increased, the points ω_1 and ω_2 approach each other and are annihilated, and there remains a single interval of one solution and one of three solutions, separated by the point ω_3 . We will call this threshold the ω_1 - ω_2 bifurcation. On the other hand, increasing μ or decreasing γ brings the points ω_2 and ω_3 together, resulting in a single interval

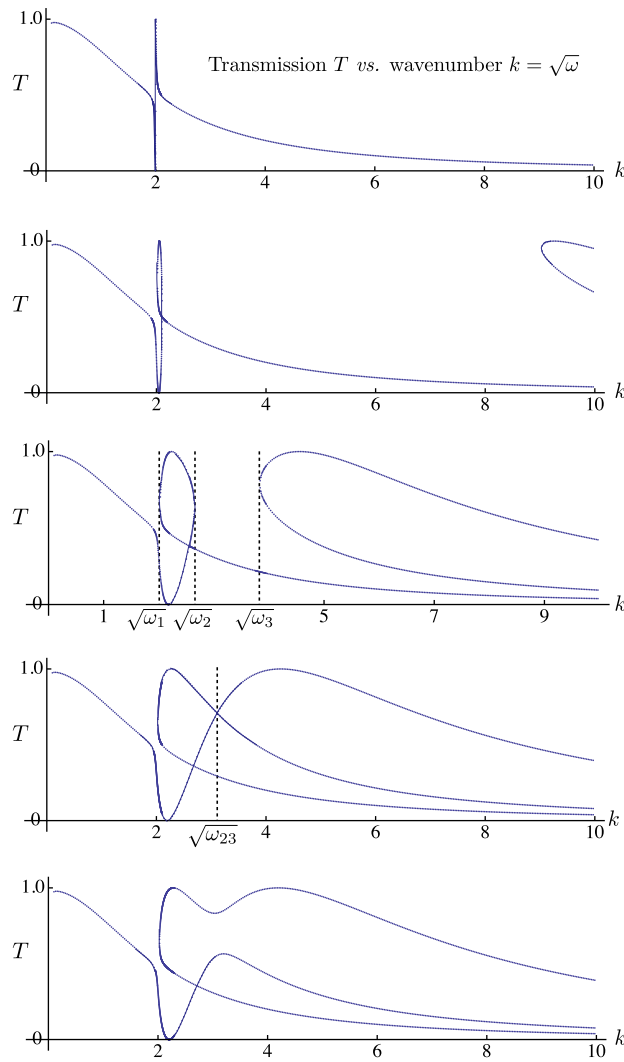


Figure 3. The transmission coefficient $T := |B/J|^2$ of the harmonic scattering solutions (2.2) of the string-oscillator system (1.1) versus the wavenumber $k = \sqrt{\omega}$. The graphs show a progression of values of the composite nonlinearity parameter $\mu = \lambda J^2$ (from top to bottom, $\mu = 0, 0.001, 0.0035, 0.003856, 0.00395$), all other parameters being fixed ($E_0 = 4, \gamma = 0.3$). The top graph shows the linear case, in which each frequency admits a single harmonic solution. The sharp anomaly occurs near the characteristic frequency $E_0 = 4$ of the oscillator. For nonzero μ , there is a half-infinite frequency interval (ω_3, ∞) of triple solutions. As μ increases (or as γ decreases), a narrow frequency interval (ω_1, ω_2) of triple solutions emerges; this is the ω_1 - ω_2 bifurcation. Meanwhile, ω_3 decreases, eventually merging with ω_2 and eliminating the interval (ω_2, ω_3) of unique solutions; this is the ω_2 - ω_3 bifurcation. A diagram of the bifurcations for this progression is shown in figure 4 (bottom).

$[\omega_1, \infty)$ of multiple solutions. We call the threshold that occurs when they are annihilated the ω_2 - ω_3 bifurcation.

Each of these bifurcations is analysed in detail in the following section, and table 1 is a summary of the results. Asymptotically, as μ and γ vanish, the bifurcations are characterized by specific power laws. The ω_1 - ω_2 bifurcation occurs at relatively weak nonlinearity, $\mu \sim C\gamma^4$,

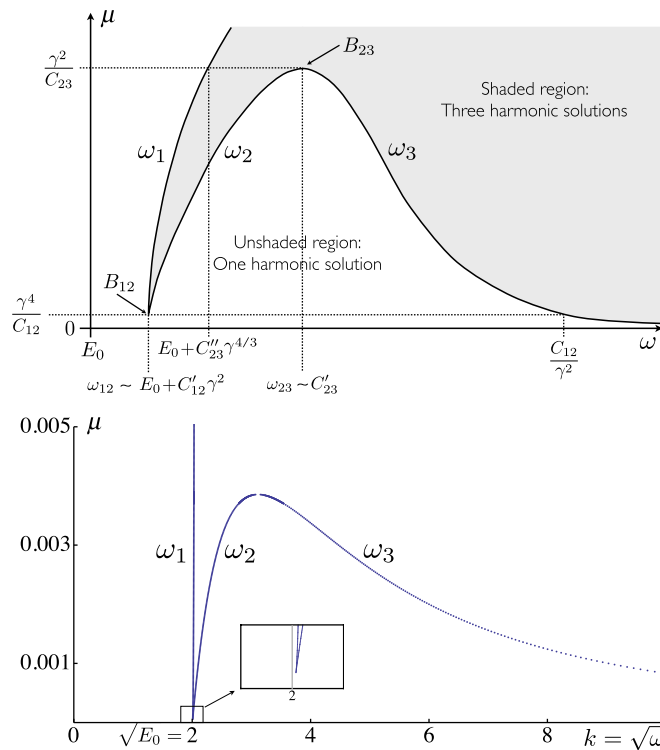


Figure 4. Top: this diagram describes the emergence of a frequency band of multiple solutions which eventually merges with the high-frequency band of multiple solutions as the composite nonlinearity parameter $\mu = \lambda J^2$ increases with the coupling γ fixed. It shows the transition frequencies ω_1 , ω_2 and ω_3 , versus μ , at which the number of harmonic scattering solutions of the form (2.2) changes from 1 to 3 or vice versa, according to whether the cubic polynomial (2.8) for the response has one or three real roots. The unshaded region indicates those (ω, μ) pairs that admit only one real root, whereas pairs in the lightly shaded region admit three real roots. Bifurcations occur at the points B_{12} (the cuspidal ω_1 - ω_2 bifurcation in the text) and B_{23} (ω_2 - ω_3 bifurcation) as μ varies. The coordinates of the two bifurcations are labelled with their asymptotic values for small γ and μ , according to table 1. Bottom: this is a numerical computation for $E_0 = 4$ and $\gamma = 0.3$ that corresponds to figure 3.

Table 1. Asymptotics of the bifurcations of the transition frequencies for small γ and μ . The bifurcation diagram with μ as the bifurcation parameter and fixed γ is shown in figure 4. All constants depend only on E_0 and are computed explicitly in the text. The three relations in the first row are given in equations (3.24)–(3.26); the relations in the second row are given in equations (3.31), (3.34) and (3.30).

Bifurcation	Power law	ω_1	ω_2	ω_3
$\omega_1 = \omega_2$	$\frac{\gamma^4}{\mu} \sim C_{12}$	$\omega_{12} - E_0 \sim C'_{12} \gamma^2$		$\omega_3 \sim \frac{C_{12}}{\gamma^2}$
$\omega_2 = \omega_3$	$\frac{\gamma^2}{\mu} \sim C_{23}$	$\omega_1 - E_0 \sim C'_{23} \gamma^{4/3}$	$\omega_{23} \sim C'_{23}$	

when its effects on the resonance near E_0 first appear. The ω_2 - ω_3 bifurcation occurs at much higher values of nonlinearity relative to the coupling parameter. These constants as well as those in the asymptotics for the frequencies ω_i are computed explicitly in terms of the resonant frequency E_0 alone.

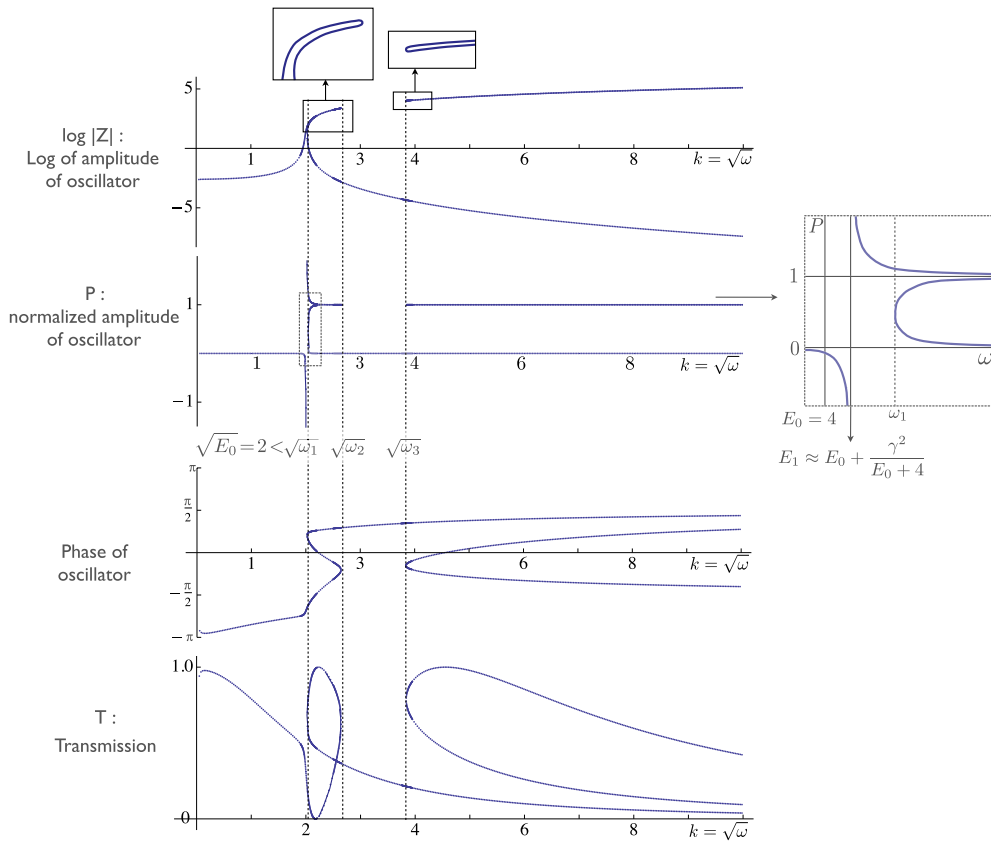


Figure 5. These graphs show the harmonic scattering states (2.2) of the string-oscillator system (1.1) versus the wavenumber $k = \sqrt{\omega}$. Plotted from top to bottom are (i) the logarithm $\log |Z|$ of the amplitude of the oscillator’s motion $z(t) = Ze^{-i\omega t}$; (ii) a rescaling P of the response $\mathcal{R} = |Z/J|^2$ defined by (2.7) (J is the amplitude of the incident field) with detail near the resonant frequency depicted to the right; (iii) the phase $\arg(Z)$ of the oscillator and (iv) the transmission coefficient $T = |B/J|^2$. For the parameter values $E_0 = 4.0$, $\gamma = 0.3$, and $\mu = 0.0035$ chosen here, there are two frequency intervals (ω_1, ω_2) and (ω_3, ∞) , delineated by the vertical dotted lines, in which the system has three solutions; at frequencies in the complementary intervals $(0, \omega_1)$ and (ω_2, ω_3) , the system has only one solution. The two high-amplitude oscillations have almost identical amplitudes, as shown in the top graph, but they differ by a phase that tends to π as $\omega \rightarrow \infty$, as seen in the third graph. A graph of the transition frequencies versus μ is shown in figure 4.

Analysis of the number of scattering solutions as a function of frequency is facilitated by a polynomial equation for the square of the amplitude enhancement $\mathcal{R} = |Z/J|^2$ in the resonator, which we call the *response*. The first equation of (2.3) yields

$$\mathcal{R} \left(\mu \mathcal{R} + \frac{\gamma^2}{\omega + 4} - (\omega - E_0) \right)^2 + \frac{4\gamma^4}{\omega(\omega + 4)^2} \mathcal{R} - \frac{4\gamma^2}{\omega + 4} = 0. \tag{2.5}$$

The roots \mathcal{R} of this equation, which are necessarily positive, are in one-to-one correspondence with the solutions (B, Z) of (2.3). A cubic equation whose solutions determine all of the possible responses of the system is due to the Kerr form of the nonlinearity; such an equation is also obtained in [13], in which the transmission line is discrete. Equation (2.5) can have

multiple roots only if

$$(\omega - E_0)(\omega + 4) - \gamma^2 > 0 \quad (\text{necessary for multiple solutions}) \quad (2.6)$$

in particular, if $\omega > E_0$, that is, if ω exceeds the frequency of the free resonator. The change of variable

$$\mathcal{R} = \frac{P}{\mu} \left(\omega - E_0 - \frac{\gamma^2}{\omega + 4} \right) \quad (2.7)$$

transforms equation (2.5) into

$$f(P) := P(P - 1)^2 + \alpha P - \beta = 0, \quad (2.8)$$

in which

$$\begin{aligned} \alpha &= \alpha(\omega; \gamma, E_0) := \frac{1}{\omega} \left(\frac{2\gamma^2}{(\omega - E_0)(\omega + 4) - \gamma^2} \right)^2, \\ \beta &= \beta(\omega; \gamma, \mu, E_0) := \frac{4\gamma^2\mu(\omega + 4)^2}{((\omega - E_0)(\omega + 4) - \gamma^2)^3}. \end{aligned} \quad (2.9)$$

The quantities \mathcal{R} , α , and β can be written more compactly using the notation

$$\begin{aligned} \rho &:= \omega + 4 \sim \omega && \text{as } \omega \rightarrow \infty, \\ \sigma &:= \omega - E_0 - \gamma^2/\rho \sim \omega && \text{as } \omega \rightarrow \infty. \\ \mathcal{R} &= \frac{\sigma}{\mu} P, & \alpha &= \frac{4\gamma^4}{\omega\sigma^2\rho^2}, & \beta &= \frac{4\gamma^2\mu}{\sigma^3\rho}. \end{aligned}$$

If one fixes the parameters μ , γ and E_0 of the dynamical system, one can consider the roots of the polynomial $f(P)$ as functions of frequency ω . These roots correspond to all possible responses \mathcal{R} associated with harmonic scattering solutions at ω . Transition frequencies separating unicity of the response from multiple responses occur when $f(P)$ has a double root. Thus analysis of transition frequencies is tantamount to analysis of the parameters for which $f(P)$ has a double root.

3. Multiple harmonic solutions and their bifurcations

We have seen that certain transition frequencies $\omega_i(\mu, \gamma; E_0)$ separate intervals of unique response to harmonic forcing by the source field $Je^{-i\omega t}$ from intervals of triple response. The diagram in figure 4 shows how the transition frequencies merge or separate as a function of the nonlinearity in the asymptotic regime of $\gamma \rightarrow 0$ and $\mu \rightarrow 0$. This section is devoted to proving the asymptotic power laws in that diagram. The main results are stated in the following theorem.

Theorem 3.1. *The transition frequencies ω_i that separate frequency intervals of unique scattering solutions from intervals of multiple solutions vary with the nonlinearity parameter μ according to the diagram in figure 4 if the coupling parameter γ is sufficiently small. More precisely,*

1. *There are at most three transition frequencies if γ is sufficiently small.*
2. *There is a point $B_{12} = (\omega_{12}, \mu_*)$ and positive numbers C_{12} and C'_{12} with*

$$\frac{\gamma^4}{\mu_*} \sim C_{12} \quad \text{and} \quad \omega_{12} - E_0 \sim C'_{12}\gamma^2 \quad (\gamma \rightarrow 0)$$

such that, if $\mu < \mu_$, there is a single transition frequency ω_3 and if $\mu > \mu_*$ but μ is not too large, there are three transition frequencies with $\omega_1 < \omega_2 < \omega_3$. As $\mu \rightarrow \mu_*$*

from above, $\omega_1 \rightarrow \omega_{12}$ and $\omega_2 \rightarrow \omega_{12}$. Moreover when $\mu = \mu_*$, there are two transition frequencies $\omega_{12} = \omega_1 = \omega_2 < \omega_3$ and

$$\omega_3 \sim \frac{C_{12}}{\gamma^2} \quad (\gamma \rightarrow 0) \quad (\omega_1 = \omega_2).$$

The numbers C_{12} and C'_{12} depend only on E_0 and are given by (3.24) and (3.25).

3. There is a point $B_{23} = (\omega_{23}, \mu^*)$ and positive numbers C_{23} and C'_{23} with

$$\frac{\gamma^2}{\mu^*} \sim C_{23} \quad \text{and} \quad \omega_{23} \sim C'_{23} \quad (\gamma \rightarrow 0)$$

such that, if $\mu > \mu^*$, there is a single transition frequency ω_1 and if $\mu < \mu^*$ but μ is not too small, there are three transition frequencies with $\omega_1 < \omega_2 < \omega_3$. As $\mu \rightarrow \mu^*$ from below, $\omega_2 \rightarrow \omega_{23}$ and $\omega_3 \rightarrow \omega_{23}$. Moreover, when $\mu = \mu^*$, there are two transition frequencies $\omega_1 < \omega_2 = \omega_3 = \omega_{23}$ and

$$\omega_1 - E_0 \sim \frac{3}{C_{23}^{1/3}} \gamma^{4/3} \quad (\gamma \rightarrow 0).$$

The numbers C_{23} and C'_{23} depend only on E_0 and are given by (3.31) and (3.30).

The transition frequencies are characterized by the property that there exists a real number P such that both (2.8) and its derivative with respect to P vanish. The system of the two conditions is algebraically equivalent to the pair

$\begin{aligned} \alpha(\omega; \gamma, E_0) &= -3(P - \frac{1}{3})(P - 1), \\ \beta(\omega; \gamma, \mu, E_0) &= -2P^2(P - 1). \end{aligned}$	(conditions for transition frequencies) (3.10)
--	--

It is convenient to work with the roots of $\sigma\rho = (\omega - E_0)(\omega + 4) - \gamma^2 = (\omega - E_1)(\omega + c)$, which are small perturbations of E_0 and -4 as $\gamma \rightarrow 0$,

$$(\omega - E_1)(\omega + c) = (\omega - E_0)(\omega + 4) - \gamma^2, \tag{3.11}$$

$$E_1 = E_0 + \epsilon, \tag{3.12}$$

$$c = 4 + \epsilon, \tag{3.13}$$

$$\epsilon = \frac{\gamma^2}{E_0 + 4} + \mathcal{O}(\gamma^4), \tag{3.14}$$

$$a = 4 + E_1 = 4 + E_0 + \epsilon. \tag{3.15}$$

Because of inequality (2.6), multiple solutions are possible only for $\omega > E_1$, and we therefore introduce the variables

$$v = \omega - E_1, \tag{3.16}$$

$$\tau = v^{-1}, \tag{3.17}$$

$$q = 3P - 2. \tag{3.18}$$

The algebraic system (3.10) in P and ω can be rewritten as a system in q and τ :

$$(1 - q)(1 + q) = 3\alpha = 12\gamma^4 \frac{\tau^5}{(1 + E_1\tau)(1 + (a + \epsilon)\tau)^2},$$

$$(1 - q)(2 + q)^2 = \frac{27}{2}\beta = \frac{54\gamma^2\mu\tau^4(1 + a\tau)^2}{(1 + (a + \epsilon)\tau)^3}.$$

Dividing the second by the first and retaining the first equation yields the equivalent pair

$$(1 - q)(1 + q) = 12\gamma^4 \frac{\tau^5}{(1 + E_1\tau)(1 + (a + \epsilon)\tau)^2} = \frac{12\gamma^4}{v^2(v + E_1)(v + (a + \epsilon))^2}, \tag{3.19a}$$

$$\frac{(2 + q)^2}{1 + q} = \frac{9}{2} \frac{\mu}{\gamma^2} \frac{(1 + a\tau)^2(1 + E_1\tau)}{\tau(1 + (a + \epsilon)\tau)} = \frac{9}{2} \frac{\mu}{\gamma^2} \frac{(v + a)^2(v + E_1)}{v(v + (a + \epsilon))}. \tag{3.19b}$$

3.1. Graphical depiction of transition frequencies and their bifurcations

These two algebraic relations between q and τ are shown in figures 7 and 8; the symmetric one is (3.19a). They provide a transparent graphical means of analysing the transition frequencies and their bifurcations. The τ -values of the points of intersection between the two relations determine these frequencies through $\omega = E_1 + \tau^{-1}$. It is visually clear that there are at most three intersection points, and we give a proof of this in section 3.5. Figure 7 shows the evolution of the relations as μ increases, for a fixed value of γ . Initially, there is a single intersection, corresponding to ω_3 . At a critical value of μ , another intersection appears at the top, which then splits into two intersections corresponding to ω_1 ($q < 0$) and ω_2 ($q > 0$). This is the ω_1 - ω_2 bifurcation. After a mountain-pass mutation of relation (3.19b), the intersection points corresponding to ω_2 and ω_3 approach each other, fuse together, and then disappear on the lower right half of relation (3.19a) in the ω_2 - ω_3 bifurcation.

When γ tends to zero, the peak of relation (3.19a) grows without bound. But the frequency of the ω_2 - ω_3 bifurcation remains of order 1 and (3.19a) appears as two practically vertical lines, one at $q = -1$ and one at $q = 1$. This regime is depicted in figure 8.

The graphical realizations of relations (3.19a) and (3.19b) in figures 7 and 8 are obtained as follows. In (3.19a), the function of τ maps the positive real line onto itself in a strictly increasing manner. Thus τ is implicitly a function of $q \in (0, 1)$ with infinite slope at $q = \pm 1$, and we denote this symmetric function by $\tau = \mathcal{T}(q)$.

Relation (3.19b) can be understood by placing the graphs of the functions

$$f_1(q) = \frac{(2 + q)^2}{1 + q}, \tag{3.20}$$

$$f_2(\tau) = \frac{9}{2} \frac{\mu}{\gamma^2} \frac{(1 + a\tau)^2(1 + E_1\tau)}{\tau(1 + (a + \epsilon)\tau)}, \tag{3.21}$$

side by side, as shown in figure 6. The function f_1 is convex and tends to infinity as $q \rightarrow -1$ or $q \rightarrow \infty$; its minimal value of 4 is achieved at $q = 0$. Likewise, f_1 is convex and tends to infinity as $\tau \rightarrow 0$ or $\tau \rightarrow \infty$, and thus it has a minimal value, say m_0 . If $m_0 < 4$, then (3.19b), or $f_1(q) = f_2(\tau)$, has two components, each of which is the graph of a function of q , one with unique local maximum τ_- and the other with unique local minimum τ_+ , with $\tau_- < \tau_+$, both of which are achieved at $q = 0$. If $m_0 > 4$, then each of two components is the graph of a function of τ , the lower having maximal value q_- and the upper having minimal value q_+ , with $q_- < 0 < q_+$. At the transition from one regime to the other, when $m_0 = 4$, the relation consists of two curves crossing tangentially at $q = 0$.

If τ is viewed as a multi-valued function of q , then the upper branch of (3.19b) is decreasing for $q < 0$ and increasing for $q > 0$. Since (3.19a) has the opposite behaviour, it intersects the upper branch of (3.19b) either not at all, exactly once at $q = 0$, or at two points, one with $q < 0$ and one with $q > 0$. One can see that the τ -value of the former is larger by the observation that $f_1(-q) - f_1(q) = 2q^3/(1 - q^2) > 0$, for $q \in (0, 1)$. It is clear from the graphs that the lower branch intersects (3.19a) at most once, and only for $q > 0$; a rigorous statement is proved in section 3.5.

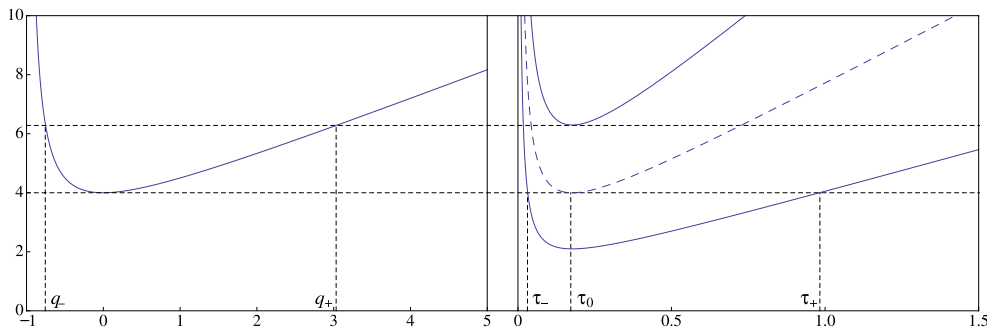


Figure 6. The concave functions $f_1(q)$ and $f_2(\tau)$ in relation (3.19b). The function $f_1(q)$ does not depend on the parameters of the system, whereas $f_2(\tau)$ does. When the minimal value of f_2 is less than that of f_1 (equal to 4), the relation $f_1(q) = f_2(\tau)$ possesses two components that are functions of q , with minimal and maximal τ -values equal to τ_- and τ_+ , as in the first three graphs of figure 7. When $\min f_2(\tau) > 4$, the two components are functions of τ , with minimal and maximal τ -values equal to q_- and q_+ as in the last three graphs of figure 7.

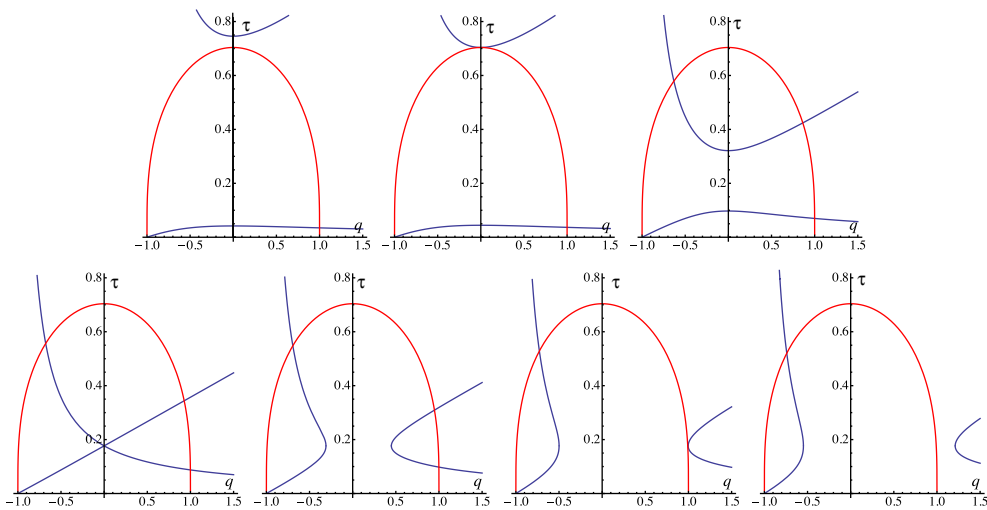


Figure 7. Relations (3.19a) and (3.19b) in the (q, τ) plane, whose intersections give the transition frequencies through $\omega = E_1 + \tau^{-1}$. The symmetric one is (3.19a). The values of γ and E_0 are fixed, and the graphs from left to right show the evolution of relation (3.19b) as μ increases. The two bifurcations occur at the tangential intersections, as in the second (ω_1 - ω_2 bifurcation) and sixth (ω_2 - ω_3 bifurcation) graphs.

3.2. The ω_1 - ω_2 bifurcation

We first analyse the bifurcation occurring at the point B_{12} of figure 4, at which a narrow frequency interval of multi-valued harmonic solutions is born as μ increases across a threshold value (with γ fixed). We prove the power law $\gamma^4 \sim C_{12}\mu$ and the asymptotics of the transition frequencies at this bifurcation. The sharp feature in the bifurcation at the point B_{12} is in fact cuspidal with $\omega_2 - \omega_1 \sim C(\mu - \mu_0)^{3/2}$, meaning that the (ω_1, ω_2) interval opens slowly.

The maximal value of the function $\tau = T(q)$ is attained at $q = 0$, and we denote it by

$$\tau_* = \nu_*^{-1} = \max_{q \in (0,1)} T(q) = T(0).$$

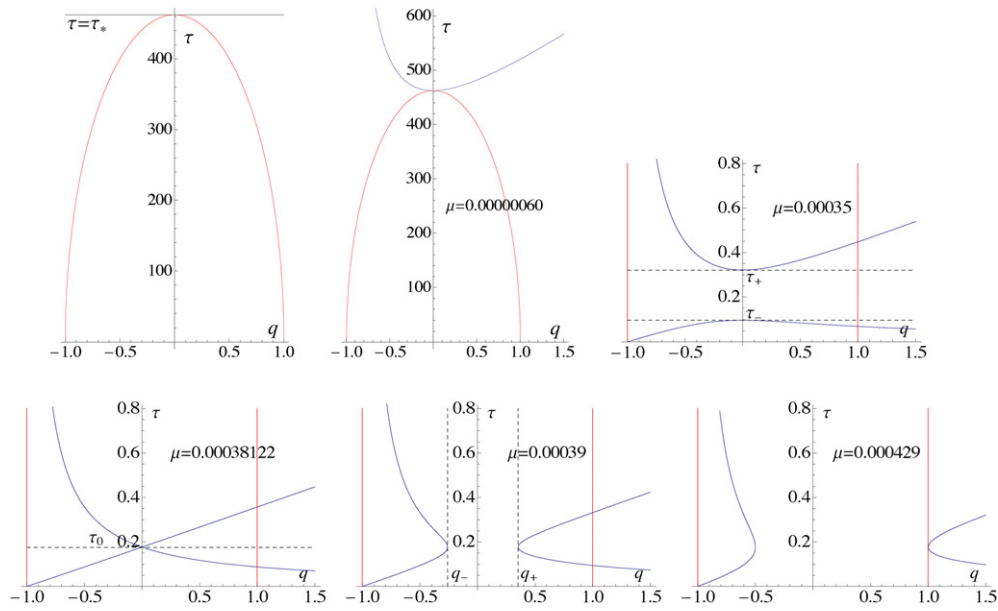


Figure 8. Relations (3.19a) and (3.19b) for small γ and μ . The intersections of the two relations correspond to the transition frequencies. Here, $\gamma = 0.1$ and $E_0 = 4$, and μ increases through values ranging from the ω_1 - ω_2 bifurcation at $\mu \sim \gamma^4/C_{12} \approx \gamma^4/166 \approx 6.0e-7$, through the crossing at $\mu \sim \gamma^2/C \approx \gamma^2/26.2 \approx 0.00038122$, to the ω_2 - ω_3 bifurcation at $\mu \sim \gamma^2/C_{23} \approx \gamma^2/23.3 \approx 0.000429$.

Setting $q = 0$ in (3.19a) and (3.19b) gives

$$12\gamma^4 = v_*^2(v_* + E_1)(v_* + a + \epsilon)^2.$$

As $\gamma \rightarrow 0$ with $v_* > 0$, we have $v_* \rightarrow 0$, $v_* + E_1 \rightarrow E_0$, and $v + a + \epsilon \rightarrow E_0 + 4$, and thus

$$\frac{12\gamma^4}{v_*^2} \rightarrow E_0(E_0 + 4)^2 \quad (\gamma \rightarrow 0),$$

from which we obtain

$$\tau_* \sim \frac{\sqrt{E_0(E_0 + 4)}}{2\sqrt{3}\gamma^2} = \frac{C_*}{\gamma^2} \quad (\gamma \rightarrow 0). \tag{3.22}$$

The pair of frequencies ω_1 and ω_2 is born (or annihilated) when the upper branch of the second relation in (3.19a) and (3.19b) intersects the first relation $\tau = T(q)$ at its peak, that is, when $\tau_+ = \tau_*$, as shown in the middle top graph of figure 8.

The numbers τ_{\pm} are the solutions of the second relation of (3.19a) and (3.19b) with $q = 0$. This equation can be written as

$$\eta \frac{8\gamma^2}{9\mu} \tau = (1 + a\tau)(1 + E_1\tau),$$

in which

$$\eta := \frac{1 + a\tau + \epsilon\tau}{1 + a\tau} = 1 + \epsilon \frac{\tau}{1 + a\tau}, \quad 0 < \frac{\tau}{1 + a\tau} < \frac{1}{E_0 + 4},$$

so that $\eta \rightarrow 1$ as $\gamma \rightarrow 0$. Thus we obtain

$$aE_1\tau^2 + \left(a + E_1 - \eta \frac{8\gamma^2}{9\mu}\right) \tau + 1 = 0. \tag{3.23}$$

Setting $\tau = \tau_*$ in this equation, with $\gamma \rightarrow 0$, the asymptotic relation $\tau_* \sim C_*/\gamma^2$ yields the balance of two terms,

$$\eta \frac{8}{9} \frac{\gamma^2 C_*}{\mu \gamma^2} \sim a E_1 \frac{C_*^2}{\gamma^4} \quad (\omega_1 = \omega_2, \gamma \rightarrow 0),$$

which results in the asymptotic power law for the ω_1 - ω_2 bifurcation

$$\boxed{\frac{\gamma^4}{\mu} \sim \frac{3\sqrt{3}}{16} E_0^{3/2} (E_0 + 4)^2 =: C_{12} \quad (\omega_1 = \omega_2, \gamma \rightarrow 0).} \tag{3.24}$$

Let us denote by $\omega_{12} = \omega_1 = \omega_2$ the frequency at which this bifurcation takes place. Equation (3.22) and the definitions of ν and τ give $\omega_{12} - E_0 - \epsilon \sim \gamma^2/C_*$, and this together with $\epsilon \sim \gamma^2/(4 + E_0)$ yields

$$\boxed{\omega_{12} - E_0 \sim \gamma^2 \left(\frac{1}{C_{12}} + \frac{1}{4 + E_0} \right) = \gamma^2 \frac{2\sqrt{3} + \sqrt{E_0}}{\sqrt{E_0}(E_0 + 4)} = \gamma^2 C'_{12} \quad (\gamma \rightarrow 0).} \tag{3.25}$$

As this bifurcation takes place, the third transition frequency ω_3 is very large, and one can compute its asymptotic value by finding the intersection between $\tau = T(q)$ and the lower branch of the second relation of (3.19a) and (3.19b). Let us denote this intersection by (q_3, τ_3) . The maximal τ -value of the lower branch is τ_- , which satisfies (3.23), and is seen to be of order $\mathcal{O}(\gamma^2)$, and thus the first equation of (3.19a) and (3.19b) gives $q = 1 + \mathcal{O}(\gamma^{16})$. Inserting this into the second of (3.19a) and (3.19b), gives

$$\eta \tau_3 = \frac{\gamma^2}{C_{12}} (1 + a \tau_3)(1 + E_1 \tau_3),$$

in which $\eta \rightarrow 1$ as $\gamma \rightarrow 0$, or

$$1 + \left(a + E_1 - \frac{C_{12}}{\gamma^2} \eta \right) \tau + a E_1 \tau^2 = 0,$$

which has a solution $\tau_3 \sim \gamma^2/C_{12}$. Finally, $\omega_3 = \tau_3^{-1} + E_1$, which yields

$$\boxed{\omega_3 \sim \frac{C_{12}}{\gamma^2} \quad (\omega_1 = \omega_2, \gamma \rightarrow 0).} \tag{3.26}$$

The response \mathcal{R}_{12} of the field at the frequency ω_{12} tends to infinity as γ^{-2} . This can be seen by inserting the asymptotic expressions (3.24) and (3.25) into (2.7) with $q = 0$:

$$\mathcal{R}_{12} = \left(\omega_{12} - E_0 - \frac{\gamma^2}{\omega_{12} + 4} \right) \frac{2}{3\mu} \sim \frac{1}{\gamma^2} \frac{3}{4} E_0 (E_0 + 4).$$

Similarly, the response of the field that is created or annihilated at the transition frequency ω_3 , that is, the field corresponding to the double root of (2.8), is found to be

$$\mathcal{R}_3 \sim \frac{2}{3} \frac{C_{12}}{\mu^2} \sim \frac{2}{3} \frac{C_{12}^3}{\gamma^8} \quad (\omega_1 = \omega_2, \gamma \rightarrow 0).$$

Let us see why the ω_1 - ω_2 bifurcation is a cusp. It occurs when a convex function and a concave function intersect tangentially at their extreme values, as seen the second graph of the sequences in figures 7 and 8. The concave function is symmetric and the convex one is not. Up to order $\mathcal{O}(q^3)$, these functions can be represented by

$$\tau = \tau_0 - cq^2, \quad r > 0, \quad c > 0, \tag{3.27}$$

$$\tau = \tau_0 - r\delta + aq^2 + bq^3, \quad a > 0, \tag{3.28}$$

in which ϵ is a rescaling of μ . After making the substitutions $r\delta/(a+c) \mapsto \delta$ and $d = b/(a+c)$, the intersection points (q, τ) of these two relations satisfy

$$\delta = q^2(1 + dq).$$

The small solutions of this equation have an expansion in powers of $\sqrt{\delta}$,

$$q_{1,2} = \pm \delta^{1/2} - \frac{d}{2}\delta \pm \frac{5}{8}d^2\delta^{3/2} + \dots,$$

and the corresponding τ -coordinates are

$$\tau_{1,2} = -c\delta \pm d\delta^{3/2} + \dots.$$

The difference of these is

$$\tau_1 - \tau_2 = 2d\delta^{3/2}.$$

Seeing that $\tau = 1/(\omega - E_1)$ and δ is a rescaling of μ , the difference $\omega_2 - \omega_1$ is of order $(\mu - \mu_0)^{3/2}$.

3.3. Between bifurcations

The structural morphosis of the relation $f_1(q) = f_2(\tau)$ occurs when the minima of f_1 and f_2 are equal and is characterized by the crossing of two curves at $(0, \tau_0)$ as depicted in figures 6 and 8. The number τ_0 is where f_2 attains its minimum value, say $f_2(\tau_0) = m_0$. By writing

$$f_2(\tau) = \frac{(1 + (E_0 + 4)\tau)(1 + E_0\tau)}{\tau}\eta(\tau), \quad \eta(\tau) = \frac{1 + a\tau}{1 + (a + \epsilon)\tau},$$

in which $\eta(\tau) - 1$ and $\eta'(\tau)$ are both $\mathcal{O}(\gamma^2)$ uniformly in τ , one finds that

$$\tau_0 \sim \frac{1}{\sqrt{E_0(E_0 + 4)}} \quad (\gamma \rightarrow 0)$$

and that

$$m_0 := f_2(\tau_0) \sim 9\frac{\mu}{\gamma^2} \left(2 + E_0 + \sqrt{E_0(E_0 + 4)}\right) \quad (\gamma \rightarrow 0).$$

The crossing occurs when $q = 0$ and $\tau = \tau_0$ simultaneously in the relation $f_1(q) = f_2(\tau)$, that is, when $4 = m_0$, which yields the asymptotic power law

$$\boxed{\frac{\gamma^2}{\mu} \rightarrow \frac{9}{4} \left(2 + E_0 + \sqrt{E_0(E_0 + 4)}\right) \quad (\text{at crossing, } \gamma \rightarrow 0).}$$

When $m_0 < 4$, we have $\tau_- < \tau_0 < \tau_+$, where τ_{\pm} are the extremes of the two branches of the relation $f_1(q) = f_2(\tau)$. Asymptotically,

$$\tau_- < \frac{1}{\sqrt{E_0(E_0 + 4)}} + o(\gamma) < \tau_+ \quad (\gamma \rightarrow 0).$$

When $m_0 > 4$, the extremes q_{\pm} are defined through

$$\frac{(2 + q_{\pm})^2}{1 + q_{\pm}} = m_0.$$

Since $-1 < q_- < 0$, we have $1 < (2 + q_-)^2 < 4$ and therefore

$$1 + q_- < \frac{\gamma^2}{\mu} \left(\frac{4}{9(2 + E_0 + \sqrt{E_0(E_0 + 4)})} + o(\gamma) \right) < 4(1 + q_-).$$

The point (q_-, τ_0) is the rightmost point on the left branch of the relation $f_1(q) = f_2(\tau)$, and from the diagrams in figure 8, this point is evidently to the right of the graph of $\tau = \mathcal{T}(q)$,

as the latter is practically a vertical line at $q = -1$ when τ is of order 1. The value of q that satisfies $\mathcal{T}(q) = \tau_0$ is obtained by setting $\tau = \tau_0$ in the first equation of (3.19a) and (3.19b):

$$(1 - q)(1 + q) = \gamma^4 \left(\frac{12}{E_0^{3/2}(E_0 + 4)^2(\sqrt{E_0} + \sqrt{E_0 + 4})^3} + o(\gamma) \right).$$

Thus $q = -1 + \mathcal{O}(\gamma^4)$ and we obtain

$$1 + q < \gamma^4 \left(\frac{6}{E_0^{3/2}(E_0 + 4)^2(\sqrt{E_0} + \sqrt{E_0 + 4})^3} + o(\gamma) \right) \quad (\mathcal{T}(q) = \tau_0, \gamma \rightarrow 0). \quad (3.29)$$

3.4. The ω_2 - ω_3 bifurcation

Because of (3.29) and the symmetry of \mathcal{T} , the two intersections for $q > 0$ merge when $q_+ = 1 + \mathcal{O}(\gamma^4)$ and $\tau \sim \tau_0$. This gives the frequency of the ω_2 - ω_3 bifurcation

$$\omega_{23} \rightarrow E_0 + \sqrt{E_0(E_0 + 4)} =: C'_{23} \quad (\gamma \rightarrow 0), \quad (3.30)$$

and, setting $(2 + q_+)^2/(1 + q_+) = m_0$, the asymptotic power law relating γ to μ ,

$$\frac{\gamma^2}{\mu} \sim 2 \left(2 + E_0 + \sqrt{E_0(E_0 + 4)} \right) =: C_{23} \quad (\omega_2 = \omega_3, \gamma \rightarrow 0). \quad (3.31)$$

The response at this bifurcation is obtained from (2.7),

$$\mathcal{R}_{23} \sim \frac{\sqrt{E_0(E_0 + 4)}}{\mu} = \frac{2(2 + E_0)\sqrt{E_0(E_0 + 4)} + 2E_0(E_0 + 4)}{\gamma^2}.$$

As this bifurcation takes place, the intersection that determines ω_1 has $q \rightarrow -1$ as $\gamma \rightarrow 0$. This is because, with $\gamma^2/\mu \sim C_{23}$, relation (3.19b) becomes stationary as $\gamma \rightarrow 0$, whereas relation (3.19a) contains the scaling factor γ^2 on the right-hand side. Using $\gamma \rightarrow 0$ and $q \rightarrow -1$, together with $\gamma^2/\mu \sim C_{23}$, system (3.19a) and (3.19b) gives

$$\frac{1}{1 + q} \sim \frac{9}{2C_{23}} \frac{(1 + E_0\tau)(1 + (4 + E_0)\tau)}{\tau}, \quad (3.32)$$

$$1 + q \sim 6\gamma^4 \frac{\tau^5}{(1 + E_0\tau)(1 + (4 + E_0)\tau)^2}, \quad (3.33)$$

which together yield

$$\frac{27}{C_{23}} \gamma^4 \frac{\tau^4}{(1 + (4 + E_0)\tau)} \rightarrow 1.$$

Thus $\tau \rightarrow \infty$, and we obtain

$$\tau \sim \frac{C_{23}^{1/3}}{3} \gamma^{-4/3}.$$

Using now $\omega_1 - E_0 + \mathcal{O}(\gamma^2) = \tau^{-1}$, we obtain

$$\omega_1 - E_0 \sim \frac{3}{C_{23}^{1/3}} \gamma^{4/3} \quad (\omega_2 = \omega_3, \gamma \rightarrow 0). \quad (3.34)$$

The response at the transition frequency ω_1 , corresponding to the double root of (2.8), is $\mathcal{R}_1 = (\omega_1 - E_0 + \mathcal{O}(\gamma^2))/(3\mu)$, which results in

$$\mathcal{R}_1 \sim \frac{2}{3} \frac{C_{23}^{2/3}}{\gamma^{2/3}}.$$

3.5. Proof of at most three transition frequencies

This section contains the proof of part (1) of theorem 3.1. It can be reformulated as follows.

Proposition 1. *System (3.19a) and (3.19b), or, equivalently, system (3.10), has at most two solutions with $0 \leq q < 1$ ($\frac{2}{3} \leq P < 1$), and if μ and γ are sufficiently small, then the system has at most one solution with $-1 < q \leq 0$ ($\frac{1}{3} < P \leq \frac{2}{3}$).*

Using the relations $3\alpha = 1 - q^2$ and $27\beta/2 = 4 - 3q^2 - q^3$, system (3.19) can be written equivalently as

$$\begin{aligned} q^2 &= \frac{12\gamma^4}{v^2(v + E_1)(v + (a + \epsilon))^2}, \\ \frac{2q^2}{1 + q} &= 9 \frac{\mu}{\gamma^2} \frac{(v + E_1)(v + a)^2}{v(v + (a + \epsilon))} - 8, \end{aligned} \tag{3.35}$$

and the first shows that $|q| < 1$.

First we deal with $0 \leq q < 1$. Setting G and H equal to the right-hand-sides of the first and second equations of (3.35) gives G as an increasing function of v that maps $(0, \infty)$ onto $[-\infty, 1)$ and thus H is a well-defined function of $G \in (-\infty, 1)$. One computes that

$$\frac{d^2H}{dG^2} = \left(\frac{dG}{dv}\right)^{-2} \left[\frac{d^2H}{dv^2} - \frac{d^2G}{dv^2} \frac{dH}{dv} \left(\frac{dG}{dv}\right)^{-1} \right]$$

and that $d^2H/dv^2 > 0$, $d^2G/dv^2 < 0$ and $dG/dv > 0$ (for $v > 0$). Thus, whenever $dH/dv > 0$, $d^2H/dG^2 > 0$ also. Since

$$\frac{dH}{dG} = \frac{dH}{dv} \left(\frac{dG}{dv}\right)^{-1} \quad \text{and} \quad \frac{dG}{dv} > 0,$$

we see that $d^2H/dG^2 > 0$ whenever $dH/dG > 0$.

Let v_0 be the positive value of v that corresponds to $G = 0$, so that $[v_0, \infty)$ maps onto the G -interval $[0, 1)$. Since H is a convex function of v that tends to infinity as $v \rightarrow 0$ or $v \rightarrow \infty$, it has a unique local minimum on $[v_0, \infty)$ (possibly at v_0), and thus H has a unique local minimum as a function of G (possibly at $G = 0$); denote this function by $H = \mathcal{H}(G)$.

The expressions $G = q^2$ and $H = 2q^2/(1 + q)$ for $q \in [0, 1)$ constitute a parametrization of the relation $H = 2G/(1 + \sqrt{G})$ for $G \in [0, 1)$, in which H is an increasing concave function of G . It remains to count the number of intersections between $H = \mathcal{H}(G)$ and $H = 2G/(1 + \sqrt{G})$ on the G -interval $[0, 1)$. Since $\mathcal{H}(G)$ has a unique local minimum and is convex whenever it is increasing, it intersects $H = 2G/(1 + \sqrt{G})$ no more than twice.

Now let us consider $-1 < q \leq 0$. Let $\tau = F(q)$ be defined through the relation $f_1(q) = f_2(\tau)$ for $q \in (0, q_-)$ ($q_- \leq 0$) and $\tau < \tau_0$. We shall show that, for γ sufficiently small and $\mu = \text{const.}\gamma$, we have $F''(q) > 0$, $1 + q_- > \text{const.}\gamma$, and $T(q) = \tau_0 \implies 1 + q = \mathcal{O}(\gamma^4)$. From this, it follows that the relation $f_1(q) = f_2(\tau)$ intersects $\tau = T(q)$ exactly once for $q < 0$ and these values of γ and μ . The result is extended to $\mu < \mathcal{O}(\gamma)$ by the observation that, as μ decreases, q_- increases (until it reaches 0) and $F(q)$ decreases, which disallows the occurrence of any additional intersections (figure 9).

We have already found that $\tau_0 \sim 1/\sqrt{E_0(E_0 + 4)}$, that $1 + q_- > \text{const.}\gamma^2/\mu$, and that $\tau_0 = T(p) \implies 1 + q_- < \text{const.}\gamma^4$ as $\gamma \rightarrow 0$. Define

$$g_1(q) = \frac{1}{f_1(q)}, \quad g_2(\tau) = \frac{\tau}{(1 + E_0\tau)(1 + (E_0 + 4)\tau)},$$

so that $F(q)$ satisfies the asymptotic relation

$$g_1(q) \sim \frac{\gamma^2}{\mu} g_2(F(q)) \quad (\gamma \rightarrow 0).$$

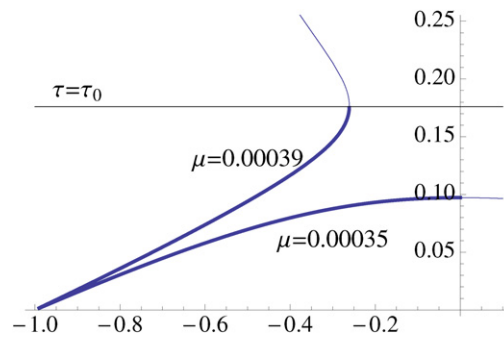


Figure 9. The function $\tau = F(q)$ in the proof in section 3.5, representing the lower branch for $q < 0$ of the relation (3.19b). It is increasing as a function of μ and convex if $\mu = \text{const.}\gamma$ and γ is sufficiently small.

The second derivative of F satisfies asymptotically

$$F''(q) \sim \frac{1}{g_2'(q)} \left(g_1''(q) - \frac{\mu}{\gamma^2} \frac{g_1'(q)}{g_2'(q)} g_2''(q) \right) \quad (\tau = F(q)).$$

One can verify the following for (q, τ) on the graph of F : $g_2'(q) > 0$, $g_1''(q)$ is bounded from below; $g_2''(q)$ is negative and bounded from above; if $q_- < 0$, then $g_1'(q)/g_2'(q)$ is positive and bounded from below (in fact this ratio reaches ∞ at $q = q_-$, where $g_2'(q) = 0$). As we have seen, we can guarantee $q_- < 0$ by making $\mu = \text{const.}\gamma$, and then, if γ is sufficiently small, we obtain $F''(q) > 0$.

4. Stability of harmonic solutions

To analyse the stability of the harmonic scattering solutions of the form (2.2), we first project the system to the resonator. This results in an equation for z alone exhibiting dissipation in the form of a delayed response coming from the coupling to the Schrödinger string with a point-mass defect. We then linearize about harmonic solutions $Ze^{-i\omega t}$. Linear stability analysis is carried out by analysing the determinant $D(s)$ of this linear system in the Laplace-transform variable s in the regime of small γ and μ . Any zero of $D(s)$ in the right half plane indicates linear instability, whereas all zeroes being in the left half plane indicates linear stability.

The responses $|Z/J|^2$ are obtained from the roots of the polynomial $f(P)$ (2.7), (2.8), and it is the roots P themselves that appear in the expression for $D(s)$. When γ and μ are small and $\omega - E_0$ is bounded from below, one root of f is very close to zero, and when there are three roots, two of them are very close to 1 (figure 10, top). For the highest and lowest responses, the real parts of all zeroes of $D(s)$ are shown to have a very small negative real part asymptotically as $\gamma \rightarrow 0$ and $\mu \rightarrow 0$. A precise statement in terms of $D(s)$ is made in section 4.4, and the result is the following theorem.

Theorem 2.

1. The harmonic response corresponding to the lowest root of the polynomial $f(P)$ is linearly stable for $\omega - E_0 > 0$ if γ and μ are sufficiently small.
2. When the system admits three distinct harmonic scattering solutions (necessarily $\omega - E_0 > 0$) and if γ and μ are sufficiently small, then
 - a. the solution corresponding to the middle root is linearly unstable;
 - b. the solution corresponding to the highest root is linearly stable if ω is large enough and linearly unstable if $E_0 < \omega < 1/2$.

Part (2b) has an intriguing consequence. If γ and μ are small enough and chosen such that the ratio μ/γ^2 is large enough, there is a single frequency interval (ω_1, ∞) of triple harmonic solutions for which the highest response is unstable for small frequencies and stable for large frequencies. Thus a transition from instability to stability occurs at some frequency.

Let us assume that, for $t \leq 0$, the system is in a harmonic scattering state $(u_h(x, t), y_h(t), z_h(t))$ of the form (2.2). The state is perturbed for $t > 0$ by forcing the resonator by a small-amplitude, temporally localized function $\varepsilon(t)$. Make the following substitutions in the main system (1.1):

$$u(x, t) = u_h(x, t) + v(x, t),$$

$$y(t) = y_h(t) + \eta(t),$$

$$z(t) = z_h(t) + \zeta(t).$$

The deviation $(v(x, t), \eta(t), \zeta(t))$ of the solution from the harmonic one vanishes at $t = 0$, as does $\varepsilon(t)$, and it satisfies the system

$$iv_t + v_{xx} = 0 \quad \text{for } x \neq 0, \tag{4.36}$$

$$i\dot{\eta} = \gamma\zeta - (v_x(0^+, t) - v_x(0^-, t)) \quad \text{with } \eta(t) = v(0, t), \tag{4.37}$$

$$i\dot{\zeta} = E_0\zeta + \gamma\eta + \lambda(2|z_h|^2\zeta + z_h^2\bar{\zeta} + 2z_h|\zeta|^2 + \bar{z}_h\zeta^2 + |\zeta|^2\zeta) + \varepsilon(t). \tag{4.38}$$

In addition, we impose on v an outgoing condition as $|x| \rightarrow \infty$, discussed below; see (4.42). This outgoing condition postulates decay of the $v(x, t)$ as $|x| \rightarrow \infty$. It is symmetric in x because (i) v starts at rest ($v(x, 0) \equiv 0$), that is, u is a pure harmonic solution for $t < 0$ and (ii) the value $v(0, t)$ together with the requirement of decay determines $v(x, t)$ for both $x \rightarrow \infty$ and $x \rightarrow -\infty$.

4.1. The outgoing condition

The outgoing condition is understood through consideration of an auxiliary problem on the half-line $x \geq 0$ without forcing and with a free endpoint at $x = 0$,

$$\begin{aligned} ia &= -a_{xx}, & x > 0, & t > 0, \\ a(x, 0) &= 0, & x \geq 0 & \quad \text{(initially at rest),} \\ a(x, t) &\rightarrow 0 & \text{as } x \rightarrow \infty, & t \geq 0 \quad \text{(decaying at } \infty). \end{aligned} \tag{4.39}$$

The Laplace transform of this system is $is\hat{a} = -\hat{a}_{xx}$ with $\hat{a}(s, x) \rightarrow 0$ as $x \rightarrow \infty$. The solution satisfies $\hat{a}_x = i^{3/2}\sqrt{s}\hat{a}$, with $\arg(i^{3/2}) = 3\pi/4$, branch cut of $\sqrt{}$ on the negative half-line, and $\text{Re}\sqrt{s} > 0$, or

$$\hat{a}(x, s) = \hat{a}(0, s) e^{i^{3/2}\sqrt{s}x} \quad (x \geq 0). \tag{4.40}$$

The inverse Laplace transform gives the general solution in terms of the Laplace-transformed value of $a(0, t)$,

$$a(x, t) = \frac{1}{2\pi i} \int_{-i\infty+0}^{i\infty+0} \hat{a}(0, s) e^{i^{3/2}\sqrt{s}x} e^{st} ds.$$

The part of the integral along $s = -i\omega + 0$ ($\omega > 0$) is a superposition of radiating (outward travelling) waves, and the part along $s = i\omega + 0$ ($\omega > 0$) is a superposition of spatially evanescent fields.

An analogous argument gives the outgoing condition for a function $b(x, t)$ defined for $x \leq 0$:

$$\hat{b}(x, s) = \hat{b}(0, s) e^{-i^{3/2}\sqrt{s}x} \quad (x \leq 0), \tag{4.41}$$

which is equivalently expressed as $\hat{b}_x = -i^{3/2}\sqrt{s}\hat{b}$.

The value of $v(0, t)$ connects $v(x, t)$ to the left of the defect ($x < 0$) continuously with $v(x, t)$ to the right of the defect ($x > 0$), that is, one puts $\hat{a}(0, s) = \hat{v}(0, s) = \hat{b}(0, s)$ in (4.40) and (4.41). Thus the outgoing condition for the perturbation v is expressed in the Laplace variable by

$$\hat{v}_x(x, s) = \begin{cases} -i^{3/2}\sqrt{s} \hat{v}(x, s) & \text{for } x < 0, \\ i^{3/2}\sqrt{s} \hat{v}(x, s) & \text{for } x > 0, \end{cases} \quad (\text{outgoing condition}) \quad (4.42)$$

in which $\arg(i^{3/2}) = 3\pi/4$ and $\hat{v}(x, s)$ is continuous in x . In fact, $\hat{v}(x, s)$ is completely determined by $\hat{v}(0, s)$.

4.2. Reduction of the system to the resonator

Because of (4.42), v is spatially symmetric, that is, $v(x, t) = v(-x, t)$, and the jump in its derivative at $x = 0$ can be expressed in a simple way:

$$v_x(0^+, t) - v_x(0^-, t) = 2v_x(0^+, t). \quad (4.43)$$

Through the outgoing condition (4.42), this is expressed in the Laplace variable by

$$\mathcal{L}[v_x(0^+, t) - v_x(0^-, t)] = 2i^{3/2}\sqrt{s} \hat{\eta}. \quad (4.44)$$

Equation (4.37) now yields a relation between η and ζ ,

$$\eta(t) = \gamma \mathcal{L}^{-1}[\hat{g}(s)\hat{\zeta}](t) = \gamma(g * \zeta)(t), \quad (4.45)$$

in which

$$\hat{g}(s) = \frac{-i}{s + 2\sqrt{is}} \quad (4.46)$$

with the branch cut for $\sqrt{\cdot}$ on the negative real half-axis and $\sqrt{r} > 0$ for $r > 0$. Relation (4.45) allows one to project the system onto the resonator by considering equation (4.38) for a single function ζ ,

$$i\dot{\zeta} = E_0\zeta + \gamma^2(g * \zeta) + \lambda(2|z_h|^2\zeta + z_h^2\bar{\zeta} + 2z_h|\zeta|^2 + \bar{z}_h\zeta^2 + |\zeta|^2\zeta) + \varepsilon(t). \quad (4.47)$$

The real part of the function $\hat{g}(s)$ is positive for s in the right half plane, which is a condition for power dissipation for a linear system ($\lambda = 0$ here) discussed in [5].

4.3. Linearization about a harmonic solution

Equation (4.47) is linearized by eliminating the quadratic and cubic terms in ζ and replacing $\zeta(t)$ with the solution $\xi(t)$ of the resulting linear equation. It is convenient to remove the oscillatory factor $e^{-i\omega t}$ and deal with the field $\psi(t) = \xi(t)e^{i\omega t}$. Keeping in mind that $z_h = Ze^{-i\omega t}$, one arrives at the following equation for ψ :

$$i\dot{\psi} = (E_0 - \omega)\psi + \gamma^2 p * \psi + \lambda(2|Z|^2\psi + Z^2\bar{\psi}) + \varepsilon(t)e^{i\omega t}, \quad (4.48)$$

in which $p(t) = g(t)e^{i\omega t}$. In the Laplace variable, this becomes

$$(is + \omega - E_0 - \gamma^2\hat{p} - 2\lambda|Z|^2)\hat{\psi} - \lambda Z^2\hat{\bar{\psi}} = \hat{\varepsilon}|_{s-i\omega}, \quad (4.49)$$

$$(-is + \omega - E_0 - \gamma^2\hat{\bar{p}} - 2\lambda|Z|^2)\hat{\bar{\psi}} - \lambda\bar{Z}^2\hat{\psi} = \hat{\varepsilon}|_{s+i\omega}. \quad (4.50)$$

The second equation is obtained by conjugating the first, replacing s with \bar{s} , and then using the rule $\hat{\bar{f}}(s) = \hat{f}(\bar{s})$ for $\text{Re}(s) > 0$. All quantities are analytic in s within their domains of definition. The determinant of this system is

$$D(s) = 3\lambda^2|Z|^4 - 4\lambda|Z|^2(\omega - E_0 - \gamma^2(\widehat{\text{Re } p})) + (-is + \omega - E_0 - \gamma^2\hat{\bar{p}})(is + \omega - E_0 - \gamma^2\hat{p}), \quad (4.51)$$

in which

$$\hat{p}(s) = \frac{1}{\omega + is + 2i\sqrt{\omega + is}}, \tag{4.52}$$

$$\hat{\tilde{p}}(s) = \frac{1}{\omega - is - 2i\sqrt{\omega - is}}. \tag{4.53}$$

The branch cut in the argument of the square root in the denominator of \hat{p} is taken to be the negative imaginary axis and the branch is defined by $\sqrt{1} = 1$; this imparts a branch cut in the s variable along the half-line $\{s = s_1 + i\omega, s_1 \leq 0\}$ in the left half plane. Enforcing the rule that $\hat{\tilde{p}}(s) = \hat{\tilde{p}}(\bar{s})$ for $\text{Re}(s) > 0$ dictates that the branch cut for the argument of the square root in $\hat{\tilde{p}}$ is the positive imaginary axis with $\sqrt{1} = 1$; this imparts a branch cut in s along the half-line $\{s = s_1 - i\omega, s_1 \leq 0\}$. Thus $D(s_1 + is_2)$ has two branch cuts along the half-lines $\{s = s_1 \pm i\omega, s_1 \leq 0\}$.

With these stipulations of the square roots, the denominator of \hat{p} vanishes at the single point $s = i\omega$ and the denominator of $\hat{\tilde{p}}$ vanishes at the single point $s = -i\omega$.

4.4. Stability analysis

This section is dedicated to the proof of theorem 2, which is stated in the proposition below in terms of the roots of $D(s)$.

The linear stability of the system about a scattering solution u_h , that is, whether $\psi(t)$ grows or decays as $t \rightarrow \infty$, depends on the roots of $D(s)$. Any root in the right half s -plane indicates exponential growth, and all roots being in the left half plane indicates decay. In terms of the quantity $P = \mu R / \sigma = \lambda |Z|^2 / \sigma$, with $\sigma = \omega - E_0 - \gamma^2 / (\omega + 4)$, D has the form

$$D = 3P^2 - 4P \frac{1}{\sigma} \left(\omega - E_0 - \frac{\gamma^2}{2} (\hat{p} + \hat{\tilde{p}}) \right) + \frac{1}{\sigma^2} (\omega - E_0 - is - \gamma^2 \hat{\tilde{p}}) (\omega - E_0 + is - \gamma^2 \hat{p}). \tag{4.54}$$

Thus $D(s)$ depends explicitly on the parameters ω , P , and γ^2 (as well as E_0). The value of P is related to u_h through the correspondence between harmonic solutions and real roots of the polynomial $f(P) := P(P - 1)^2 + \alpha P - \beta$ (2.8), which depends parametrically on γ , μ , and ω . When α and β are small, the smallest root P_1 is nearly zero and, in the case of three roots, the other two P_1 and P_2 are nearly 1.

Proposition 3.

1. In expression (4.54) for D , let P be equal to the smallest root of $f(P)$. If $\omega - E_0 > 0$ is bounded from below and γ and μ are sufficiently small, then all zeroes of $D(s)$ have (small) negative real part.
2. Suppose that $f(P)$ has three roots (necessarily $\omega > E_0$).
 - a. In (4.54), let P be set to the intermediate root. If γ and μ are sufficiently small, then $D(s)$ has a root with positive real part.
 - b. In (4.54), let P be set to the largest root. If the conditions

$$\begin{aligned} \omega &> \frac{1}{2} \\ (\omega^2 - 1)(\omega - E_0)^2 &> \omega^2 \\ \frac{4\gamma^2\mu}{(\omega - E_0)^3(\omega + 4)} &\ll |1 - P| \ll 1 \\ \frac{\mu}{\gamma^2} &> \frac{\omega - E_0}{\omega(\omega + 4)} \end{aligned}$$

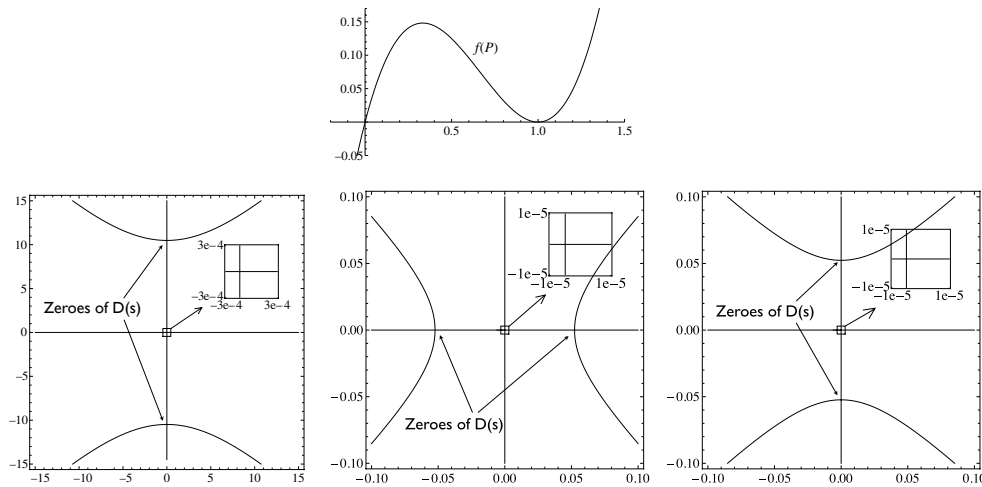


Figure 10. Top. Each of the three roots P_i , $i = 1, 2, 3$ of the polynomial $f(P) = P(P - 1)^2 + \alpha P - \beta$ (2.8), all of which are positive, corresponds to a harmonic solution of the system (1.1). The response of resonator is related to P by equation (2.7). With the parameters $\gamma = 0.05$, $\mu = 4\gamma^2/C_{23} \approx 0.000429$, and $E_0 = 4$, and $\omega = 1.5\omega_{23} \approx 14.5$, P_1 is very close to 0, whereas $P_{2,3}$ are very close to 1. (There is only one transition frequency ω_1 for these parameters, i.e. μ is above the point B_{23} in figure 4.) Bottom. For each root P_i , the zero sets of the real and imaginary parts of $D(s)$ (4.54) in the complex s -plane are shown from left to right in increasing order of P_i . These graphs only show the zeros of $D(s)$ that are away from $\pm i\omega$. For γ sufficiently small, the imaginary part of D vanishes on the real axis and on an almost vertical curve approximately connecting the points $-i\omega$ and $i\omega$, whereas the real part vanishes on a hyperbola-like curve. The real part of this curve is small and negative, in agreement with the asymptotic calculation in section 4.4 when \hat{p} or $\hat{\bar{p}}$ is bounded.

are satisfied and if γ and μ are sufficiently small, all zeroes of $D(s)$ have (small) negative real part. If $E_0 < \omega < 1/2$, then $D(s)$ has a zero with (small) positive real part.

Let us simplify notation by putting

$$\begin{aligned} \rho &= \omega + 4, & \sigma &= \omega - E_0 - \gamma^2/\rho, \\ \alpha &= \frac{4\gamma^4}{\omega\sigma^2\rho^2}, & \beta &= \frac{4\gamma^2\mu}{\sigma^3\rho}, \\ P &= 1 + Q. \end{aligned}$$

Case $P \ll 1$. We assume that $\omega - E_0 > 0$ is bounded from below and let γ and μ tend to zero. In this regime, $\sigma \sim \omega - E_0$, so $1/\sigma = \mathcal{O}(1)$. Definition (2.9) of α and β show that these quantities vanish as $\gamma, \mu \rightarrow 0$, and thus the smallest root P_1 of $f(P) := P(P - 1)^2 + \alpha P - \beta$ is asymptotic to β :

$$P \sim \beta = \frac{4\gamma^2\mu}{\sigma^3\rho} = \mathcal{O}(\gamma^2\mu). \tag{4.55}$$

Case $P \ll 1$ and $\hat{p}, \hat{\bar{p}}$ bounded. The first two terms of (4.54) vanish in this regime, and thus the third term also vanishes, yielding two cases,

$$(\omega - E_0 - is - \gamma^2\hat{p}) \rightarrow 0 \quad \text{or} \quad (\omega - E_0 + is - \gamma^2\hat{\bar{p}}) \rightarrow 0. \tag{4.56}$$

Putting $s = s_1 + is_2$ in the first case yields

$$s_2 \sim -(\omega - E_0) < 0, \tag{4.57}$$

$$s_1 \sim -\gamma^2 \text{Im } \hat{p}. \tag{4.58}$$

The sign of $-\text{Im } \hat{p}$ is the same as that of $-\text{Re}(s_1 + 2\sqrt{\omega - is_1 + s_2})$. This latter expression is asymptotic to $-\text{Re}(2\sqrt{\omega + s_2}) \sim -2\sqrt{E_0}$. This quantity is negative by the declaration of the square root in the definition of g (4.46). Thus s_1 is asymptotically negative. A similar argument for the second of the cases (4.56) shows that $s_2 \sim \omega - E_0 > 0$ and that $s_1 \sim \gamma^2 \text{Im } \hat{p} < 0$. Thus the roots s of $D(s) = 0$ are in the left half plane.

Case $P \ll 1$ and \hat{p} or $\hat{\bar{p}}$ unbounded. As we have mentioned at the end of section 4.3, the denominator of \hat{p} vanishes only at $i\omega$ and that of $\hat{\bar{p}}$ only at $-i\omega$. Thus, if one of these quantities is unbounded, the other remains bounded. It suffices to analyse the case of \hat{p} being unbounded, as $\hat{\bar{p}}(s) = \overline{\hat{p}(\bar{s})}$ and $D(\bar{s}) = \overline{D(s)}$.

If $\text{Re}(s) > 0$, then $\sqrt{\omega + is}$ is in the upper half plane. The square root in the definition (4.52) of \hat{p} takes arguments in the upper half plane into the first quadrant, and thus

$$\text{Re}(s) > 0 \implies \text{Im}\sqrt{\omega + is} > 0. \tag{4.59}$$

We will prove that this condition is asymptotically inconsistent with $D(s) = 0$.

The assumption that $\hat{p} \rightarrow \infty$ implies $s \rightarrow i\omega$. Applying this to the three terms of $D(s)$ in (4.54) gives

$$\begin{aligned} D &= \frac{48\gamma^4\mu^2}{\sigma^6\rho^2}(1 + o(1)) - \frac{16\gamma^2\mu}{\sigma^4\rho} \left(\sigma - \frac{\gamma^2}{2}\hat{p} \right) (1 + o(1)) \\ &\quad + \frac{2\omega - E_0}{\sigma^2} (E_0(1 + o(1)) - \gamma^2\hat{p}) (1 + o(1)) \\ &= \gamma^2\hat{p} \left[-\frac{1}{\sigma^2}(2\omega - E_0)(1 + o(1)) + \frac{8\gamma^2\mu}{\sigma^2\rho}(1 + o(1)) \right] \\ &\quad + \frac{1}{\sigma^2}(2\omega - E_0)E_0(1 + o(1)) \\ &\quad - \frac{16\gamma^2\mu}{\sigma\rho}(1 + o(1)) + \frac{48\gamma^4\mu^2}{\sigma^4\rho^2}(1 + o(1)) \\ &= \gamma^2\hat{p} \left(-\frac{1}{\sigma^2}(2\omega - E_0)(1 + o(1)) \right) + \frac{E_0}{\sigma^2}(2\omega - E_0)(1 + o(1)). \end{aligned}$$

Setting $D = 0$ provides the asymptotic relation

$$\hat{p} \sim \frac{E_0}{\gamma^2}.$$

On the other hand, the definition (4.52) of \hat{p} with $\omega + is \rightarrow 0$ provides the relation

$$\hat{p} \sim \frac{1}{2i\sqrt{\omega + is}}.$$

Combining these two asymptotic expressions for \hat{p} yields

$$\sqrt{\omega + is} \sim -i \frac{\gamma^2}{2E_0},$$

which, in view of (4.59), is inconsistent with $\text{Re}(s) > 0$.

Case $P \sim 1$. To see the asymptotics of the other roots, write $f(P) = 0$ in terms of $Q = P - 1$:

$$f(P) = 0 \iff Q^2 = \frac{4\gamma^4}{\sigma^3\rho} \left(\frac{\mu}{\gamma^2} (1+Q)^{-1} - \frac{\sigma}{\omega\rho} \right).$$

This implies the asymptotic

$$Q^2 \sim \frac{4\gamma^4}{\sigma^3\rho} \left(\frac{\mu}{\gamma^2} - \frac{\sigma}{\omega\rho} \right) \quad \text{when} \quad \frac{4\gamma^2\mu}{\sigma^3\rho} \ll |Q| \ll 1. \quad (4.60)$$

Thus there are two values of order γ^2 that Q can take on, one negative and one positive, under two conditions:

$$\frac{4\gamma^2\mu}{\sigma^3\rho} \ll |Q| \ll 1 \quad \text{and} \quad \frac{\mu}{\gamma^2} > \frac{\sigma}{\omega\rho} \implies Q \sim \pm C\gamma^2 (C > 0). \quad (4.61)$$

Equality in place of ' $>$ ' in the condition $\mu/\gamma^2 > \sigma/(\omega\rho)$ is achieved asymptotically at the ω_1 - ω_2 bifurcation. In general, for a fixed asymptotic ratio μ/γ^2 , the inequality is satisfied if ω is large enough or σ is small enough.

Expression (4.54) for $D(s)$ can be written as

$$\begin{aligned} D = 2Q - \frac{2\gamma^2}{\sigma\rho} + \frac{\gamma^2}{\sigma}(\hat{p} + \hat{\bar{p}}) + \frac{s^2}{\sigma^2} + \frac{is\gamma^2}{\sigma}(\hat{p} - \hat{\bar{p}}) \\ - 4Q\frac{\gamma^2}{\sigma} \left(\frac{1}{\rho} - \frac{1}{2}(\hat{p} + \hat{\bar{p}}) \right) + \frac{\gamma^4}{\sigma^2\rho^2} - \frac{\gamma^4}{\sigma^2\rho}(\hat{p} + \hat{\bar{p}}) + \frac{\gamma^4}{\sigma^2}\hat{p}\hat{\bar{p}}. \end{aligned} \quad (4.62)$$

Case $P \sim 1$ and $\hat{p}, \hat{\bar{p}}$ bounded. These assumptions imply

$$D = 2(Q + \mathcal{O}(\gamma^2)) - \frac{2\gamma^2}{\sigma\rho} + \frac{\gamma^2}{\sigma}(\hat{p} + \hat{\bar{p}}) + \frac{s^2}{\sigma^2} + \frac{is\gamma^2}{\sigma}(\hat{p} - \hat{\bar{p}}) + \mathcal{O}(\gamma^4). \quad (4.63)$$

Let us assume $Q \sim \pm C\gamma^2$ with $C > 0$ from conditions (4.61). Setting D to zero, one obtains $|s| \ll 1$, and expanding \hat{p} and $\hat{\bar{p}}$ in s gives

$$\begin{aligned} \hat{p} + \hat{\bar{p}} &= \frac{2}{\rho} - \frac{2s}{\rho\omega^{3/2}} + \mathcal{O}(|s|^2), \\ \hat{p} - \hat{\bar{p}} &= -\frac{4i}{\rho\omega^{1/2}} + \mathcal{O}(|s|). \end{aligned}$$

With these expressions, the equation $D = 0$ becomes

$$-2\sigma^2 Q (1 + \mathcal{O}(\gamma^2)) = \left(s + 2\gamma^2 \frac{\sigma(\omega - \frac{1}{2})}{\rho\omega^{3/2}} \right)^2 + \mathcal{O}(\gamma^4).$$

Because $Q \sim \pm C\gamma^2$ with $C > 0$, the $\mathcal{O}(\gamma^4)$ on the right-hand side may be absorbed into the $\mathcal{O}(\gamma^2)$ on the left-hand side,

$$s = \sqrt{-2\sigma^2 Q} - 2\gamma^2 \frac{\sigma(\omega - \frac{1}{2})}{\rho\omega^{3/2}} + \mathcal{O}(\gamma^3), \quad \sqrt{-2\sigma^2 Q} \sim c\gamma \quad (c \neq 0). \quad (4.64)$$

The negative root $Q \sim -C\gamma^2$ corresponds to the middle root P_2 of $f(P)$, or the intermediate response of the resonator depicted by the middle branch of the amplitude versus frequency graph at the top of figure 5. Thus $D(s)$ has a zero in the right half plane for sufficiently small γ .

The positive root $Q \sim C\gamma^2$ corresponds to the largest root P_3 of $f(P)$, or the highest response of the resonator depicted by the top branch of the amplitude versus frequency graph.

The first term of (4.64) is imaginary, so the second term, which is real, determines the sign of the real part of s . If $E_0 < 1/2$, then one has $\text{Re}(s) > 0$ for $\omega < 1/2$; otherwise, $\text{Re}(s) < 0$.

Case $P \sim 1$ and \hat{p} or $\hat{\tilde{p}}$ unbounded. Again, it suffices to analyse the case of \hat{p} being unbounded. Let us suppose that \hat{p} is unbounded and $\hat{\tilde{p}}$ is bounded. The balance of dominant terms in (4.62) yields

$$\frac{\gamma^2 \hat{p}}{\sigma} (1 + is) \sim -\frac{s^2}{\sigma^2}. \tag{4.65}$$

Formula (4.52) with $\hat{p} \rightarrow \infty$ gives

$$s \sim i\omega, \quad \hat{p} \sim \frac{1}{2i\sqrt{\omega + is}}.$$

Using the second of these in (4.65) gives

$$\sqrt{\omega + is} \sim -\frac{\gamma^2 \sigma (1 + is)}{2is^2},$$

and then using $s \sim i\omega$ in the right-hand side yields

$$\sqrt{\omega + is} \sim \frac{i\gamma^2 \sigma (\omega - 1)}{2\omega^2}$$

as long as $\omega \neq 1$. At $\omega = 1$, $(1 + is) = o(1)$. In any case, we obtain $\omega + is = \mathcal{O}(\gamma^4)$, so that

$$s^2 = -\omega^2 + \mathcal{O}(\gamma^4).$$

Each of the terms is and s^2 appears only once explicitly in (4.62), and they may be replaced by $-\omega$ and $-\omega^2$ committing an error of only $\mathcal{O}(\gamma^4)$. Let us also introduce the proper scaling of Q from the condition (4.61), namely $Q = \gamma^2 \tilde{Q}$:

$$D = 2\gamma^2 \tilde{Q} - \frac{2\gamma^2}{\sigma\rho} + \frac{\gamma^2}{\sigma} (\hat{p} + \hat{\tilde{p}}) - \frac{\omega^2}{\sigma^2} - \frac{\omega\gamma^2}{\sigma} (\hat{p} - \hat{\tilde{p}}) \tag{4.66}$$

$$- 4\tilde{Q} \left(\frac{\gamma^4}{\sigma\rho} - \frac{\gamma^4}{2\sigma} (\hat{p} + \hat{\tilde{p}}) \right) + \frac{\gamma^4}{\sigma^2 \rho^2} - \frac{\gamma^4}{\sigma^2 \rho} (\hat{p} + \hat{\tilde{p}}) + \frac{\gamma^4}{\sigma^2} \hat{p} \hat{\tilde{p}} + \mathcal{O}(\gamma^4). \tag{4.67}$$

Passing all terms of order γ^4 into the error (recall that $\hat{\tilde{p}} = \mathcal{O}(1)$) and rearranging terms to isolate the quantity of interest $\gamma^2 \hat{p}$ yields

$$D = \frac{\gamma^2 \hat{p}}{\sigma} \left[1 - \omega + \gamma^2 \left(2\tilde{Q} + \frac{\rho \hat{\tilde{p}} - 1}{\sigma\rho} \right) \right] - \left[\frac{\omega^2}{\sigma^2} - \gamma^2 \left(2\tilde{Q} - \frac{2}{\sigma\rho} + \frac{1}{\sigma} \hat{p} + \frac{\omega}{\sigma} \hat{\tilde{p}} \right) \right] + \mathcal{O}(\gamma^4). \tag{4.68}$$

Now setting $D = 0$ gives

$$\begin{aligned} \gamma^2 \hat{p} = & -\frac{\omega^2}{\sigma(\omega - 1)} \left[1 - \frac{\gamma^2 \sigma^2}{\omega^2} \left(2\tilde{Q} - \frac{2}{\sigma\rho} + \frac{1}{\sigma} \hat{p} + \frac{\omega}{\sigma} \hat{\tilde{p}} \right) + \mathcal{O}(\gamma^4) \right] \\ & \times \left[1 + \frac{\gamma^2}{\omega - 1} \left(2\tilde{Q} + \frac{\rho \hat{\tilde{p}} - 1}{\sigma\rho} \right) + \mathcal{O}(\gamma^4) \right]. \end{aligned} \tag{4.69}$$

The real and imaginary parts of this quantity are

$$-A := \text{Re} \gamma^2 \hat{p} = -\frac{\omega^2}{\sigma(\omega - 1)} + \mathcal{O}(\gamma^2), \tag{4.70}$$

$$\gamma^2 B := \text{Im} \gamma^2 \hat{p} = \frac{\gamma^2 \omega^2 \text{Im} \hat{\tilde{p}}}{\sigma(\omega - 1)} \left(\frac{(\omega + 1)\sigma}{\omega^2} - \frac{1}{(\omega - 1)\sigma} \right) + \mathcal{O}(\gamma^4), \tag{4.71}$$

in which \hat{p} is evaluated asymptotically using $\omega + is = \gamma^4 \xi$, where ξ is bounded:

$$\hat{p} = \frac{1}{\sqrt{2\omega - \gamma^4 \xi} (-2i + \sqrt{2\omega - \gamma^4 \xi})} \sim \frac{1}{\sqrt{2\omega} (-2i + \sqrt{2\omega})}. \quad (4.72)$$

The quantity $\gamma^2 \hat{p}$ can be evaluated alternatively directly from its definition (4.52):

$$\begin{aligned} \hat{p} &= \frac{1}{\sqrt{\omega + is} (2i + \sqrt{\omega + is})} \sim \frac{-i}{2\gamma^2 \sqrt{\xi} (1 - \frac{i}{2} \gamma^2 \sqrt{\xi})} \\ &\sim \frac{-i}{2\gamma^2 \sqrt{\xi}} \left(1 + \frac{i\gamma^2 \sqrt{\xi}}{2} - \frac{\gamma^4 \xi}{4} + \dots \right) \sim \frac{-i}{2\gamma^2 \sqrt{\xi}} + \frac{1}{4} + \frac{i\gamma^2 \sqrt{\xi}}{8} + \dots, \end{aligned}$$

which results in the asymptotic

$$\gamma^2 \hat{p} = \frac{-i}{2\sqrt{\xi}} + \frac{\gamma^2}{4} + \mathcal{O}(\gamma^4). \quad (4.73)$$

By equating expressions (4.69) and (4.73) for $\gamma^2 \hat{p}$, we obtain

$$\frac{i}{2\sqrt{\xi}} = A - i\gamma^2 B + \frac{\gamma^2}{4} + \mathcal{O}(\gamma^4) = \frac{1}{2}(\tilde{A} - i\gamma^2 \tilde{B}),$$

in which \tilde{A} and \tilde{B} are real and differ from A and B by order $\mathcal{O}(\gamma^2)$. If ω is sufficiently large, A and B are positive and bounded from below in magnitude. Specifically, it is sufficient that $(\omega^2 - 1)(\omega - E_0)^2 > \omega^2$. This yields $\text{Im } \hat{p} > 0$ asymptotically.

$$\sqrt{\xi} = \frac{-1}{2(i\tilde{A} + \gamma^2 \tilde{B})}.$$

Finally,

$$is = -\omega + \gamma^4 \xi = -\omega + \frac{\gamma^4 (\gamma^2 \tilde{B} - i\tilde{A})^2}{4 (\gamma^4 \tilde{B}^2 + \tilde{A}^2)^2},$$

which results in $\text{Im } s \sim \omega$ and

$$\text{Re } s \sim -\frac{B}{2A^3} \gamma^6.$$

This result places the zeroes of $D(s)$ asymptotically in the left half plane, regardless of the sign of Q .

5. Discussion of continuum-oscillator models

Simple continuum-oscillator systems serve a vital role in elucidating fundamental principles and phenomena in physics. Horace Lamb, interested in how disturbances in a body subside due to the transmission of energy into an infinite ambient medium devised what is now known as the Lamb model as the simplest expression of this phenomenon [8]. He showed that, if a harmonic oscillator is attached to an infinite string whose displacement is governed by the wave equation, the oscillator obeys the equation of the usual instantaneously damped harmonic oscillator. In other words, the energy loss in an oscillator due to instantaneous friction can be perfectly conceived as the radiation of energy into an infinite string. The coupled system of the oscillator and the string together is a conservative extension of the lossy system consisting of the damped oscillator alone. It is in fact the minimal conservative extension of the damped oscillator, and it is unique up to isomorphism, as shown by Figotin and Schenker [5]. The string acts as a system of ‘hidden variables’ from the point of view of an observer who is able to make measurements only of the motion of the oscillator.

The linear version ($\lambda = 0$) of our model (1.1) is designed specifically to allow the oscillator to be completely detached from the string in the zero-coupling limit ($\gamma = 0$) without severing the string. The case $\gamma = 0$ corresponds to a resonator decoupled from a system of ‘hidden’ variables that itself exhibits nonresonant scattering in a line by a point-mass defect resulting in a simple but nontrivial transmission coefficient. A very small coupling parameter $\gamma \ll 1$ corresponds to a small perturbation of a decoupled system with an embedded eigenvalue E_0 and results in a sharp resonance.

Because our transmission line is governed by a Schrödinger equation, it exhibits dispersion, which is experienced by an observer in the oscillator as a delayed response, or a noninstantaneous friction, assuming that there is no forcing originating at points along the length of the string:

$$i \dot{\zeta}(t) = E_0 \zeta(t) + \gamma^2 \int_0^\infty g(t') \zeta(t - t') dt' + \varepsilon(t) \quad (\lambda = 0),$$

$$\hat{g}(s) = \frac{-i}{s + 2\sqrt{is}}.$$

The function $g(t)$ obeys a power-dissipation condition, described in [5], which in the Laplace variable is expressed by the condition that $\hat{g}(s)$ has a positive real part when $\text{Re}(s) > 0$.

The function $\varepsilon(t)$ in the above equation is a spatially and temporally localized perturbation of a harmonic oscillation, that produces a deviation $\zeta(t)$ in the state of the oscillator. When the frequency of oscillation vanishes, the problem becomes that of the dissipation of finite-energy disturbances of a system initially at equilibrium. In this case, nonlinearities of a general form have been analysed by Komech [7] when the string’s motion is governed by the wave equation and the resonator is attached as in the Lamb model. The system exhibits transitions between stationary energies of the nonlinear potential in the resonator, which resemble transitions between energy states in atoms. In Komech’s model, the energy is related to the height of the string rather than a frequency of oscillation. A positive cubic nonlinearity has only one stationary point and all disturbances decay to zero.

At nonzero frequencies, cubic nonlinearity becomes interesting and the focus of study turns to the steady-state behaviour of a nonlinear scatterer subject to a monochromatic harmonic forcing originating from a source far away. In particular, one wants to understand how these steady oscillatory motions respond to finite-energy perturbations. Our choice of a Schrödinger equation for the string was based on the form of the nonlinearity $\lambda|z|^2z$ that is natural for this equation, and which admits periodic solutions that are purely harmonic and mathematically tractable. Perturbation about the harmonic motion $Ze^{-i\omega t}$ of the oscillator results in the equation

$$i\dot{\psi} = (E_0 - \omega)\psi + \gamma^2 \int_0^\infty p(t') \psi(t - t') dt' + \lambda(2|Z|^2\psi + Z^2\bar{\psi}) + \varepsilon(t)e^{i\omega t},$$

(4.48) for the linearized perturbed oscillation $\psi(t)e^{-i\omega t}$ of the nonlinear system. Energy loss comes from the delayed response term $\hat{p}(s) = \hat{g}(s - i\omega)$, which also satisfies the dissipation condition that $\text{Re}(s) > 0 \implies \text{Re}(\hat{p}(s)) > 0$. The solutions Z depend in a complex way on γ and λ , and stability analysis when these parameters are small is delicate, as demonstrated in section 4.

The idea of projecting a conservative oscillatory system onto a lossy subsystem is an insightful one and has been discussed from different points of view in the works mentioned above. Figotin and Schenker [5] view the whole string-oscillator system as a conservative extension of a dissipative subsystem of ‘observable variables’ (the oscillator). The string realizes in a structurally unique way a space of ‘hidden variables’ that are responsible for the

loss of energy measured by an observer confined to the oscillator. The form of the energy dissipation (as the function $g(t)$ above in the linear case) observed in the oscillator is sufficient to determine the space of hidden motions responsible for the dissipation. These ideas are brought to bear on the lossy Maxwell system in electromagnetics by these authors and others, such as Tip [19]. Komech describes the projected system as an irreversible description of a larger reversible one. This point of view had been advanced previously by Keller and Bonilla [6] as an illustration of how irreversible processes may be derived from reversible ones and was motivated by the question of whether macroscopic physical processes can be deduced from classical mechanics.

To an observer of our nonlinear system from the site of the resonator, the coupling to the string is felt as a combination of input energy and energy loss to damping. These two energies balance out (in the sense of time averages), when the system is in a harmonic steady state. The balance is disturbed when the system is perturbed from steady state. To express this perspective in precise terms, we project the system onto the resonator. Write the equation for ψ above in terms of the actual perturbation $\zeta(t) = \psi(t)e^{-i\omega t}$ of a harmonic solution $z_h = Ze^{-i\omega t}$ and reinstate nonlinear terms from (4.47):

$$\begin{aligned} i\dot{\zeta} = & E_0\zeta + \gamma^2 \int_0^\infty g(t')\zeta(t-t')dt' + \lambda(2|Z|^2\zeta + Z^2e^{-2i\omega t}\bar{\zeta}) \\ & + \lambda(2Ze^{-i\omega t}|\zeta|^2 + \bar{Z}e^{i\omega t}\zeta^2 + |\zeta|^2\zeta) + \varepsilon(t). \end{aligned}$$

Both the external forcing ε and the steady-state field $z_h = Ze^{-i\omega t}$, induced by the incident field $Je^{i(kx-\omega t)}$, affect the dynamics of the system. The field $z_h = Ze^{-i\omega t}$ depends on γ , μ , and ω through the roots of the cubic polynomial $f(P)$ (2.8). If $\varepsilon(t)$ is taken to be $\varepsilon_0\delta(t)$, where $\delta(t)$ is a unit impulse at $t = 0$, we can consider this equation for $t > 0$ with $\varepsilon = 0$ and a nonzero initial condition.

Importantly, introducing external forcing and damping through coupling to the string leads to harmonic solutions that can still be calculated explicitly. This is generally not possible if external forcing and instantaneous damping are introduced directly as in the much studied Duffing oscillator

$$\ddot{z} + a\dot{z} + E_0z + bz^3 = F_0 \cos(\omega t). \quad (5.74)$$

In spite of the similarities of cubic nonlinearity, harmonic forcing and intervals of triple solutions, these solutions are only approximately periodic in the Duffing case, when the parameters a , b and F_0 are small.

Acknowledgments

This work was supported by the National Science Foundation under grants DMS-0807325 (SPS) and DMS-0707488 (SV) while the authors were hosted at the Universidad Carlos III de Madrid in the fall of 2010. We thank the NSF and the Universidad Carlos III for their support.

References

- [1] Christ A, Tikhodeev S G, Gippius N A, Kuhl J and Giessen H 2003 Waveguide-plasmon polaritons: strong coupling of photonic and electronic resonances in a metallic photonic crystal slab *Phys. Rev. Lett.* **91** 183901
- [2] Christ A, Zentgraf T, Kuhl J, Tikhodeev S G, Gippius N A and Giessen H 2004 Optical properties of planar metallic photonic crystal structures: experiment and theory *Phys. Rev. B* **70** 125113
- [3] Cowan A R and Young J F 2003 Optical bistability involving photonic crystal microcavities and fano line shapes *Phys. Rev. E* **68** 046606
- [4] Fano U 1961 Effects of configuration interaction on intensities and phase shifts *Phys. Rev.* **124** 1866–78

- [5] Figotin A and Schenker J H 2005 Spectral theory of time dispersive and dissipative systems *J. Stat. Phys.* **118** 199–263
- [6] Keller J B and Bonilla L L 1986 Irreversibility and nonrecurrence *J. Stat. Phys.* **42** 1115–25
- [7] Komech A I 1995 On stabilization of string-nonlinear oscillator interaction *J. Math. Anal. Appl.* **196** 384–409
- [8] Lamb H 1900 On a peculiarity of the wave-system due to free vibrations of a nucleus in an extended medium *Proc. Lond. Math. Soc.* **XXXII** 208–11
- [9] Lousse V and Vigneron J P 2004 Use of Fano resonances for bistable optical transfer through photonic crystal films *Phys. Rev. B* **69** 155106
- [10] McGurn A R 2008 Transmission through nonlinear barriers *Phys. Rev. B* **77** 115105
- [11] McGurn A R and Birkok G 2004 Transmission anomalies in Kerr media photonic crystal circuits: Intrinsic localized modes *Phys. Rev. B* **69** 235105
- [12] Miroshnichenko A E, Flach S and Kivshar Y S 2010 Fano resonances in nanoscale structures *Rev. Mod. Phys.* **82** 2257–98
- [13] Miroshnichenko A E, Mingaleev S F, Flach S and Kivshar Y S 2005 Nonlinear Fano resonance and bistable wave transmission *Phys. Rev. E* **71** 036626
- [14] Pitsyna N and Shipman S P 2012 A lattice model for resonance in open periodic waveguides *Discret. Contin. Dyn. Syst.* **5** 989–1020
- [15] Shipman S P 2010 *Wave Propagation in Periodic Media: Analysis, Numerical Techniques and Practical Applications (E-Book Series: Progress in Computational Physics vol 1)* ed M Ehrhardt (Sharjah: Bentham Science Publishers) chapter 2 (Resonant Scattering by Open Periodic Waveguides)
- [16] Shipman S P, Ribbeck J, Smith K H and Weeks C 2010 A discrete model for resonance near embedded bound states *IEEE Photon. J.* **2** 911–23
- [17] Shipman S P and Venakides S 2003 Resonance and bound states in photonic crystal slabs *SIAM J. Appl. Math.* **64** 322–42
- [18] Shipman S P and Venakides S 2005 Resonant transmission near non-robust periodic slab modes *Phys. Rev. E* **71** 026611
- [19] Tip A 1998 Linear absorptive dielectrics *Phys. Rev. A* **57** 4818–41
- [20] Yanik M F, Fan S and Soljacic M 2003 High-contrast all-optical bistable switching in photonic crystal microcavities *Appl. Phys. Lett.* **83** 2739–41